

# **Automated Solar Cell Assembly Teamed Process Research**

## **Annual Subcontract Report 1 January 1993 – 31 December 1993**

M. J. Nowlan, S. J. Hogan, G. Darkazalli,  
W. F. Breen, J. M. Murach,  
S. F. Sutherland, J. S. Patterson  
*Spire Corporation  
Bedford, Massachusetts*

NREL technical monitor: H. Thomas



National Renewable Energy Laboratory  
1617 Cole Boulevard  
Golden, Colorado 80401-3393  
A national laboratory of the U.S. Department of Energy  
Operated by Midwest Research Institute  
for the U.S. Department of Energy  
under contract No. DE-AC02-83CH10093

Prepared under Subcontract No. ZAG-3-11219-01

June 1994

## NOTICE

NOTICE: This report was prepared as an account of work sponsored by an agency of the United States government. Neither the United States government nor any agency thereof, nor any of their employees, makes any warranty, express or implied, or assumes any legal liability or responsibility for the accuracy, completeness, or usefulness of any information, apparatus, product, or process disclosed, or represents that its use would not infringe privately owned rights. Reference herein to any specific commercial product, process, or service by trade name, trademark, manufacturer, or otherwise does not necessarily constitute or imply its endorsement, recommendation, or favoring by the United States government or any agency thereof. The views and opinions of authors expressed herein do not necessarily state or reflect those of the United States government or any agency thereof.

Printed in the United States of America

Available from:

National Technical Information Service

U.S. Department of Commerce

5285 Port Royal Road

Springfield, VA 22161

Price: Microfiche A01

Printed Copy A04

Codes are used for pricing all publications. The code is determined by the number of pages in the publication. Information pertaining to the pricing codes can be found in the current issue of the following publications which are generally available in most libraries: *Energy Research Abstracts (ERA)*; *Government Reports Announcements and Index (GRA and I)*; *Scientific and Technical Abstract Reports (STAR)*; and publication NTIS-PR-360 available from NTIS at the above address.



Printed on recycled paper

## TABLE OF CONTENTS

	<u>Page</u>
1 INTRODUCTION .....	1
2 TECHNICAL DISCUSSION .....	4
2.1 Process Throughput .....	5
2.2 Program Tasks .....	6
2.2.1 Task 1 - Design Definition .....	6
2.2.2 Task 2 - Cell Loading Process Development .....	8
2.2.3 Task 3 - Cell Alignment Process Development .....	13
2.2.4 Task 4 - Interconnect Ribbon Handling Process Development .....	15
2.2.5 Task 5 - Solder Flux Application Process Development .....	21
2.2.6 Task 6 - Ribbon to Cell solder Process Development .....	24
2.2.7 Task 7 - Cell String Handling Process Development .....	31
2.2.8 Task 8 - In-Line I-V String Testing Development .....	35
2.2.9 Tasks 9 and 10 - Process Subassembly Design and Test .....	38
2.2.10 Task 11 - Integrated System Design .....	39
2.2.11 Task 12 - Information Dissemination .....	40
2.3 Thin Solar Cells .....	42
3 CONCLUSIONS .....	43
4 REFERENCES .....	46
APPENDIX A - PRELIMINARY DATA SHEET SPI-ASSEMBLER™ 5000	

## LIST OF ILLUSTRATIONS

	<u>Page</u>
1	Concept for an automated solar cell tabbing and interconnecting system . . . . . 1
2	Project team organization, PVMaT Phase 3A . . . . . 2
3	Lay-out drawing of cell assembly system . . . . . 4
4	Process flow chart, solar cell assembly system. . . . . 5
5	Cell assembler capacity vs. cell efficiency for three cell sizes . . . . . 6
6	Solar cell loading options. . . . . 8
7	Lay-out of the cell loading and alignment systems. . . . . 11
8	Cell loading and aligning systems . . . . . 12
9	Xerox copy image of a Solec cell . . . . . 14
10	Components of the ribbon and cell handling system. . . . . 15
11	Photograph of the ribbon reel assembly . . . . . 17
12	Ribbon accumulator assembly lay-out drawing . . . . . 18
13	Photograph of part of the interconnect handling system. . . . . 18
14	Ribbon clamp and form assembly. . . . . 19
15	Ribbon cutter assembly with blades in the open position. . . . . 20
16	Ribbon shuttle assembly with grippers open. . . . . 21
17	Prototype ribbon flux coating subassembly with interconnect ribbon reel. . . . . 23
18	Lay-out drawing of the flux station assembly . . . . . 25
19	Photograph of the flux coating subassembly. . . . . 25
20	Two lamp solder head assembly. . . . . 26
21	Solder head actuator assembly . . . . . 27
22	Photograph of solder head and actuator assemblies . . . . . 28

## LIST OF ILLUSTRATIONS (Concluded)

	<u>Page</u>
23 Cell string conveyor assembly. . . . .	31
24 Drive pulley end of the vacuum conveyor belt . . . . .	33
25 Cell string transfer assembly . . . . .	34
26 Frame for string transfer mechanism, conveyor, I-V tester, and tables for cell string arrays (foreground) and reject strings (background) . . . . .	34
27 String transfer assembly including the 4-axis manipulator and the cell string vacuum pick-up array . . . . .	36
28 I-V tester sun simulator enclosure and lamp assembly . . . . .	37
29 Contract probe assembly, in-line I-V tester . . . . .	38
30 Cell assembler control system block diagram . . . . .	41

## LIST OF TABLES

	<u>Page</u>
I	Program tasks . . . . . 3
II	PV module manufacturers' requirements for cell interconnecting. . . . . 7
III	Cell loading with r- $\theta$ -z robot running at maximum rated speeds. . . . . 10
IV	Alignment process steps . . . . . 13
V	Flux testing summary . . . . . 24
VI	Initial process parameters for soldering cell strings . . . . . 28
VII	Solder joint pull test results. Pull angle = 45° . . . . . 29
VIII	Parameters for soldering cell strings at lower lamp power . . . . . 30
IX	Subassemblies, automated solar cell assembler . . . . . 39

## SECTION 1 INTRODUCTION

This is the first Annual Technical Progress Report for the program titled "Automated Solar Cell Assembly Teamed Process Research," funded under National Renewable Energy Laboratory (NREL) subcontract No. ZAG-3-11219-01. This report describes the work done in the period from January 6, 1993 to December 31, 1993.

This program is part of the Photovoltaic Manufacturing Technology (PVMaT) project, Phase 3A, which addresses problems that are generic to the photovoltaic (PV) industry. Crystalline silicon solar cells were used in the great majority (89%) of all terrestrial power modules shipped in 1993.<sup>1</sup> Spire's analysis in Phase 1 of the PVMaT project indicated that the use of thin ( $\leq 200 \mu\text{m}$ ) silicon cells can substantially reduce module manufacturing costs, provided that processing yields remain as high as they are now for processing standard thickness cells.<sup>2</sup> Since present solar cell tabbing and interconnecting processes have unacceptably high yield losses with such thin cells, the objective of this Phase 3A subcontract is to use Spire's light soldering technology and experience in designing and fabricating solar cell tabbing and interconnecting equipment to develop new high yield, high throughput, fully automated processes for tabbing and interconnecting thin cells. An artist's concept of this processing system is provided in Figure 1.

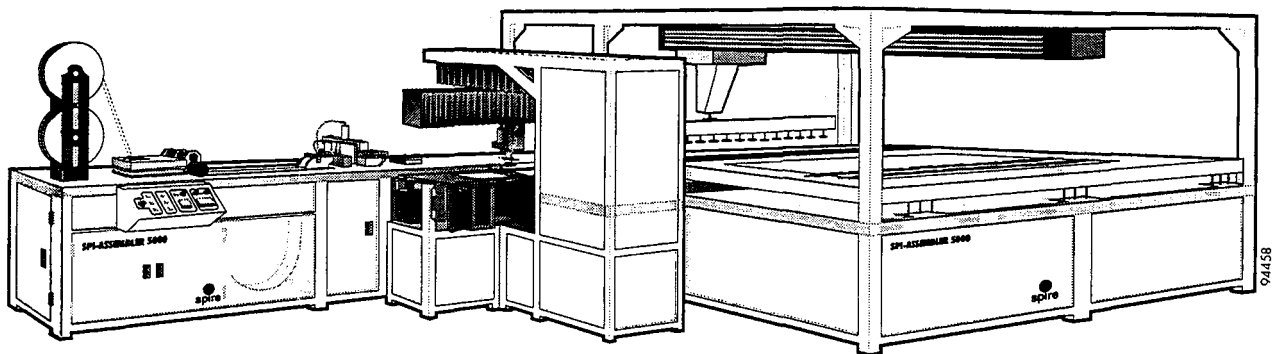


**Figure 1** *Concept for an automated solar cell tabbing and interconnecting system.*

Areas that are being addressed in this effort include processing rates, process control, yield, throughput, material utilization efficiency, and increased use of automation. Spire is teaming with Solec International, a PV module manufacturer, and the University of Massachusetts Lowell's Center for Productivity Enhancement (CPE), automation specialists, who are lower-tier subcontractors. A number of other PV manufacturers, including Siemens Solar, Mobil Solar, Solar Web, and Texas Instruments, have agreed to evaluate the processes developed under this program. A program organization chart is provided in Figure 2.

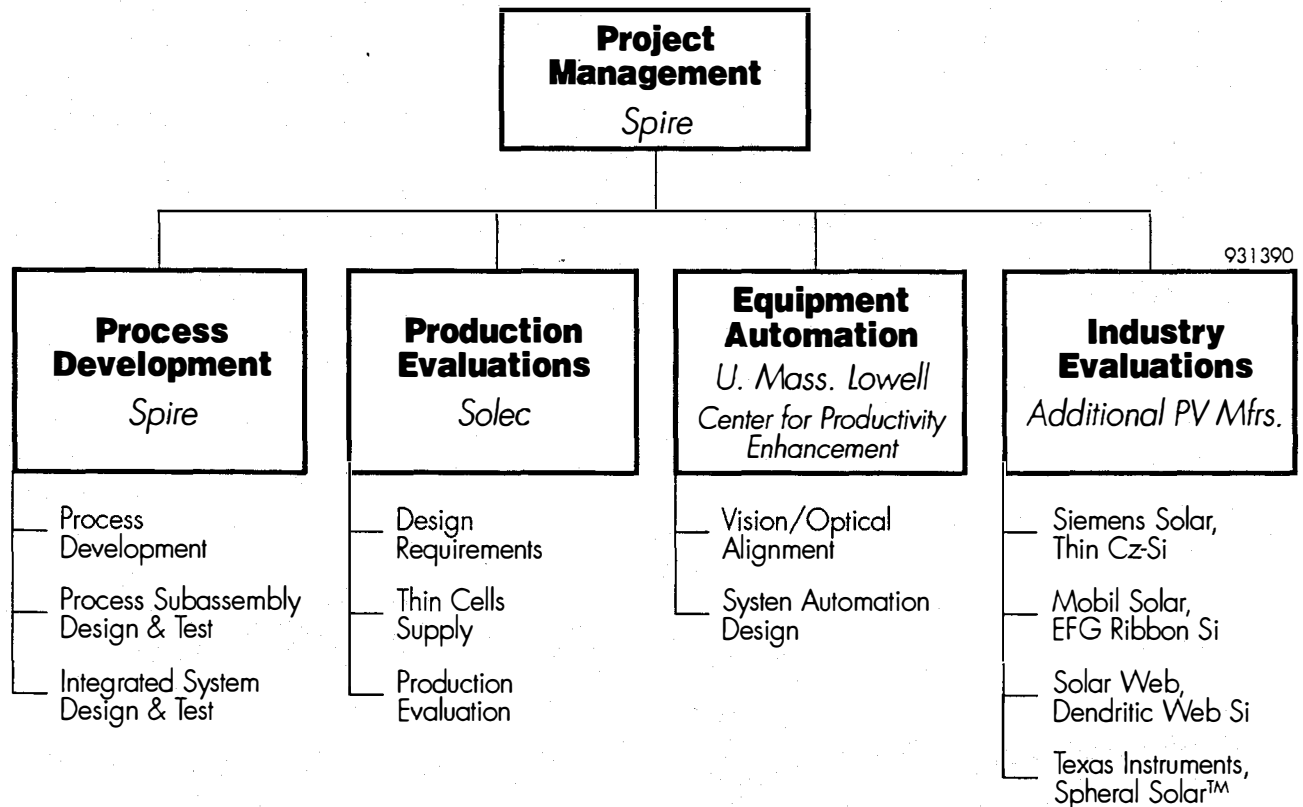


**Figure 2** *Project team organization, PVMaT Phase 3A for Automated Solar Cell Assembly Teamed Process Research.*

The program is divided into two phases with seventeen tasks. Phase I extended from January 6, 1993, to December 31, 1993, while Phase II covers efforts from December 6, 1993, to January 5, 1995. The program tasks are listed in Table I.

**Table I** *Program tasks.*

Phase	Task
I	<ol style="list-style-type: none"><li>1 Design definition</li><li>2 Cell loading process development</li><li>3 Cell alignment process development</li><li>4 Interconnect ribbon handling process development</li><li>5 Solder flux application process development</li><li>6 Ribbon to cell soldering process development</li><li>7 Cell string handling process development</li><li>8 In-line I-V string testing development</li><li>9 Process subassembly design</li><li>10 Process subassembly test</li><li>11 Integrated system design</li><li>12 Information dissemination</li></ol>
II	<ol style="list-style-type: none"><li>13 In-line I-V string testing development</li><li>14 System integration and test</li><li>15 Preliminary processing evaluation (at Spire)</li><li>16 Final processing evaluation (at Solec)</li><li>17 Information dissemination</li></ol>

## SECTION 2 TECHNICAL DISCUSSION

Spire's objective in this program is to develop high throughput (5 MW/yr) automated processes for interconnecting thin (200  $\mu\text{m}$ ) silicon solar cells. High yield will be achieved with these fragile cells through the development of low mechanical stress and low thermal stress processes. For example, a machine vision system is being developed for cell alignment without mechanical snugging, while a new soldering process is being developed to solder metal interconnect ribbons simultaneously to a cell's front and back contacts, eliminating one of the two heating steps normally used for soldering each cell. Simultaneous front and back soldering has the additional benefit of eliminating the labor intensive task of transferring tabbed cells into alignment fixtures, required for separate tabbing and interconnecting processes.

Flexible automation techniques are being incorporated wherever practical to enable the production of a variety of module designs with minimal mechanical adjustments or tooling changes. This flexibility is provided through software control of the tab length and stress-relief bend location, the number of cells per string, the number of strings per module, and the arrangement of strings in a series, parallel, or combined configuration.

The processing system will have the capacity to handle round, square, or pseudo-square (round with four large flats) cells up to 15 cm across. Strings up to 2.0m long will be assembled and arranged side-by-side to create two-dimensional module-size arrays up to 1.4m wide. A layout drawing of the system is provided in Figure 3.

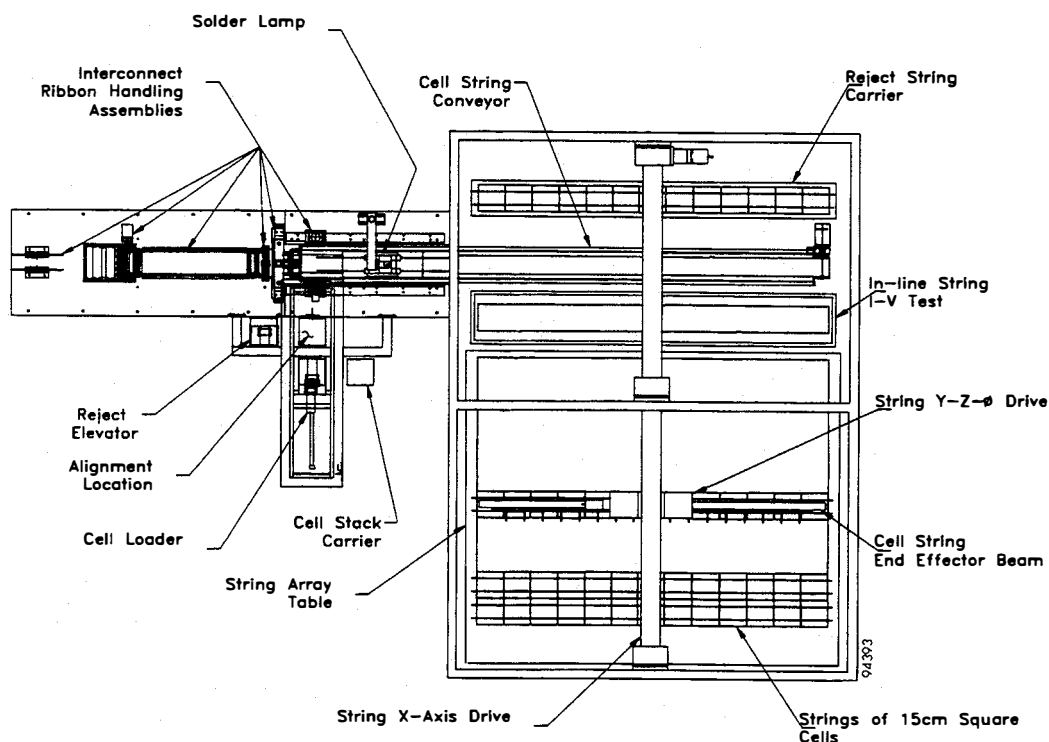


**Figure 3** Lay-out drawing of cell assembly system (plan view).

A process flow chart illustrating the flow of materials (solar cells and copper ribbon material) through the cell assembly system is shown in Figure 4.

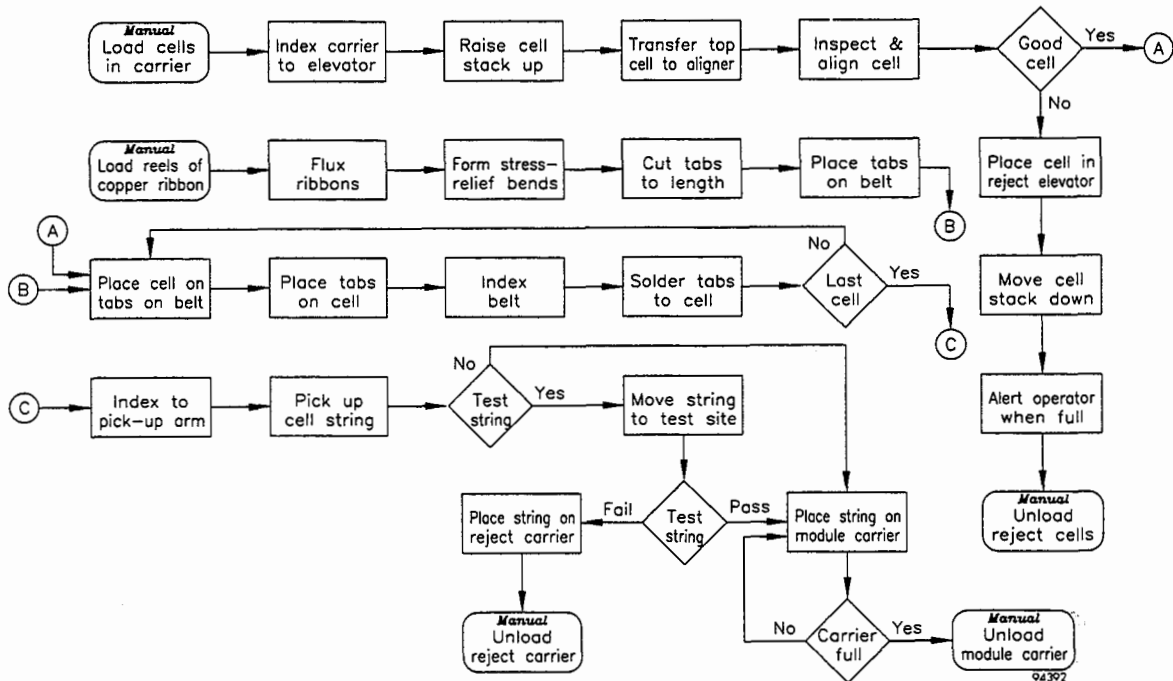


**Figure 4** Process flow chart, solar cell assembly system.

## 2.1 Process Throughput

An assembly process time budget has been created as an aid in identifying process bottlenecks or areas that may need attention to maximize system throughput. The time budget is presently in draft form, in which the step times are our current best estimates. Once the processes have been integrated, actual measured times will be recorded for each step.

Seven tasks have been identified that must satisfy the time budget. Each task is a repetitive process comprising a number of steps that must be completed within the cycle time allotted for processing a cell. To achieve high throughput, a four second per cell cycle time has been set as the nominal goal. This throughput is approximately twice as fast as Spire's current cell tabbing system, the SPI-TAB™ 1000.

The annual throughput in watts per year is a function of the processing rate, the system up-time, the cell efficiency, the cell area, the hours of operation, and the process yield. It can be calculated by the following expression:

$$T = R\eta ALn_s n_d Y$$

where

- T = annual throughput (W/yr)
- R = processing rate in cells/minute x 60 min/hr x 8 hr/shift (cells/shift)
- t = system up-time, the ratio of (operating time) / (total time)
- $\eta$  = average cell efficiency in production, Air Mass 1.5 global conditions
- A = cell area (cm<sup>2</sup>)
- L = solar insolation = 0.100 (W/cm<sup>2</sup>)
- n<sub>s</sub> = number of operating shifts per day (shifts/day)
- n<sub>d</sub> = number of operating days/week x 52 weeks/year (days/year)
- Y = process yield, the ratio of (good cells out) / (cells in)

As an example, for R = 7200, t = 75%,  $\eta$  = 12.5%, A = 100 cm<sup>2</sup>, n<sub>s</sub> = 3, n<sub>d</sub> = 260, and Y = 0.98, the annual throughput, T, is 5.16 MW/yr. This processing rate, R, is equivalent to 15 cells/minute, or a process cycle time of 4.0 s/cell, our nominal goal. Figure 5 shows the effects of cell efficiency and cell size on annual throughput. Actual values of R and Y will be measured as part of the processing evaluations scheduled for 1994.

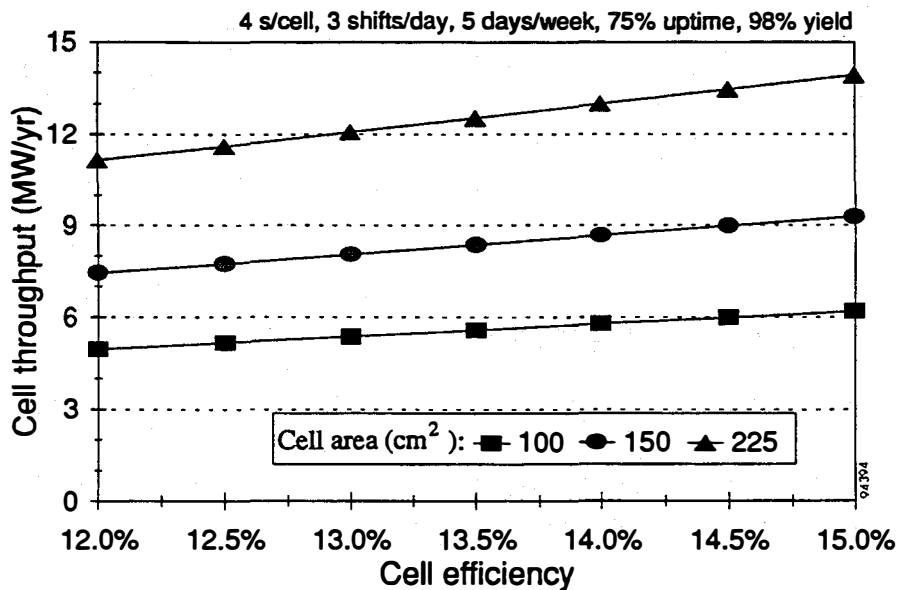


**Figure 5** Cell assembler capacity vs. cell efficiency for three cell sizes. Assumes R = 7200 cells/shift, t = 75%, n<sub>s</sub> = 3, n<sub>d</sub> = 260, and Y = 0.98.

## 2.2 Program Tasks

### 2.2.1 Task 1 - Design Definition

Spire personnel met with their lower-tier subcontractor, Solec International, in Hawthorne, CA, on March 4, 1993, to determine the specific, detailed requirements of Solec's module manufacturing line. Spire's initial concepts for manufacturing interconnected assemblies of thin (200 μm) crystalline Si solar cells were presented. Solec provided detailed input on their cell assembly requirements, including cell sizes, tab materials and geometries, solder flux, string lengths, required process yield, etc. Cell interconnection is currently an entirely manual operation at Solec.

Spire engineers also met with other PV module manufacturers to ensure that the processes developed in this program will meet the specific needs of as many manufacturers as possible. Meetings were held on March 5 with engineers at Siemens Solar Industries in Camarillo, CA, on April 6 at Spire with Mobil Solar of Billerica, MA, and on April 28 at Spire with Texas Instruments of Dallas, TX.

As with Solec, Spire presented its concepts in detail and the manufacturers provided their specific manufacturing requirements for interconnecting thin crystalline Si solar cells. The information obtained from Solec, Siemens, Mobil, and TI is being used by Spire to develop cell stringing processes that are compatible with the majority of photovoltaic module manufacturers, and that can be inserted in Solec's production line for processing evaluations in Phase II. This information on PV manufacturers' requirements is summarized in Table II.

**Table II** *PV module manufacturers' requirements for cell interconnecting.*

Category	Parameter	Requirements
Solar cell characteristics	Cell shapes Maximum cell size Cell thickness Loading arrangement	Round, square, pseudo-square, rectangular 10 to 13 cm square; 15 cm in future 200 to 450 $\mu\text{m}$ Coin stack, two for continuous feeding
Interconnect ribbon characteristics	Material Width Thickness Coating No. of ribbons/cell	Copper, ETP or OFHC <sup>a</sup> 1.5 to 2.5 mm 50 to 125 $\mu\text{m}$ Sn <sub>60</sub> Pb <sub>40</sub> or Sn 2; possibly 3 in future
Solder flux or paste requirements	Flux Paste	Low-solids "no clean" flux used with thick (12 $\mu\text{m}$ ) SnPb coating on ribbon "No clean" SnPbAg paste used with thin (1.6 $\mu\text{m}$ ) SnPb coating on ribbon
Other requirements	Maximum string length Throughput Minimum yield Minimum system up-time Pre-soldering inspection Post soldering string test	2.0m 4 to 5 s/cell 98% to 99% 75% to 80% in 3-shift 7-day operation Desirable Desirable

<sup>a</sup>ETP is electrolytic tough pitch copper, alloy C110; OFHC is oxygen-free high conductivity copper, alloy C102.

One significant recommendation which came out of these discussions is to add an in-line string I-V test to the process, after string fabrication and prior to string placement on the module carrier, as a quality control measure. Spire and NREL agreed to add two new tasks (Tasks 8 and 13) to the program to implement this in-line test.

## 2.2.2 Task 2 - Cell Loading Process Development

A process for automatically loading thin cells with high throughput is being developed under this task. A vendor survey was done to determine the availability of wafer handling equipment in the commercial marketplace. Information on wafer handling, wafer transport, and cassette handling systems was obtained and reviewed. A list of vendors was compiled to summarize and compare the types of products offered.

After reviewing the product literature, meetings were held with representatives from those companies whose handling systems seemed to be best suited for this application. Engineers from Design Technology of Billerica, MA, Monadnock Automated Design of Spofford, NH, Proconics International of Wilmington, MA, and Affiliated Manufacturers, Inc. (AMI), of North Branch, NJ, visited Spire. Extensive telephone discussions were held with Cybeq Systems of Menlo Park, CA. Spire engineers also visited Precision Robots, Inc. of Billerica, MA, and Brooks Automation of Lowell, MA. As a result of these discussions and evaluations, four general types of loading systems were defined, as illustrated in Figure 6.

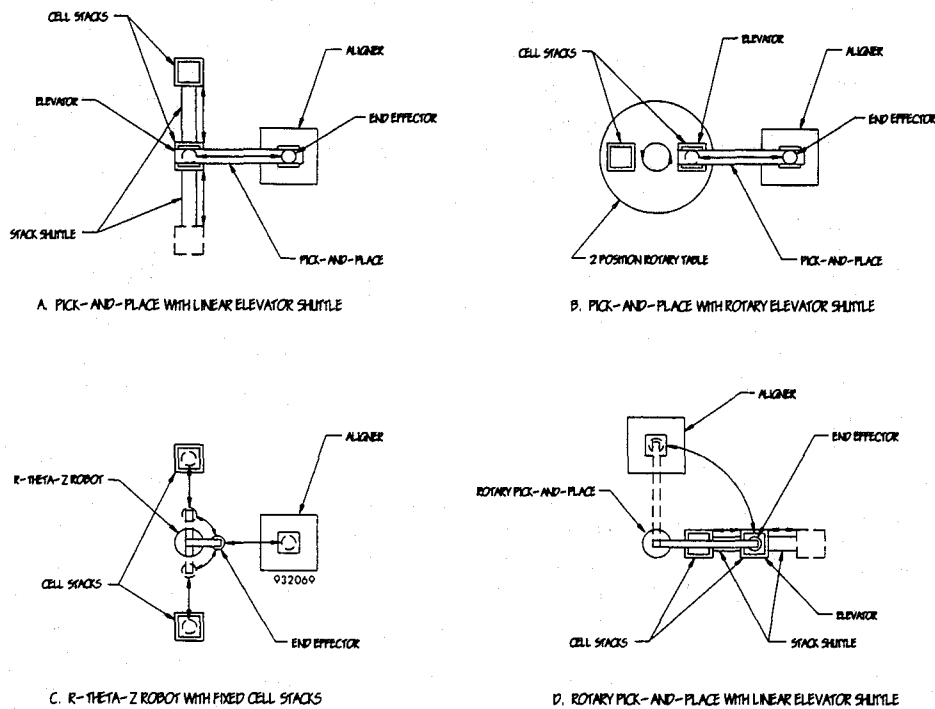


**Figure 6** Solar cell loading options.

Option A (in Figure 6) has a linear pick-and-place mechanism with x and z motions to pick up a cell from a stack elevator and place it at the aligner. Two cell stacks are mounted on a linear shuttle which transports each stack to the elevator. Option B is similar to option A except the linear shuttle is replaced with a rotary table. Option C uses an r- $\theta$ -z robot to transfer cells from fixed stacks to the aligner. In this case, no elevator is required, since the robot has sufficient z travel. Option D has a rotary pick-and-place mechanism ( $\theta$  and z motions) and a linear shuttle for cell stacks similar to option A.

Slotted cassette unloading systems, commonplace in the semiconductor industry, have been eliminated from consideration in favor of cell stack unloaders. The ability of solar cells to tolerate stacking without yield or performance degradation and the processing of cells in high volumes, on the order of millions per year, encourages PV module manufacturers to handle cells in a stack format to minimize the volume of space taken up by cells in process. For example, a typical cassette<sup>3</sup> for holding twenty-five 100 mm square wafers has overall dimensions of 14.3 cm by 12.3 cm by 11.4 cm. A stack carrier of the same dimensions can hold a stack of cells 13 cm high, equivalent to 520 cells with a thickness of 250  $\mu\text{m}$ , or more than 20 times the number of cells in the same volume. (A 250  $\mu\text{m}$  cell thickness was chosen for this example to allow 50  $\mu\text{m}$  for the front and back contacts, in addition to the silicon thickness.)

All four options (A through D) have the capacity to hold two stacks of cells to allow the operator to manually load a stack of cells while the system is automatically feeding from another stack. Thus the loading process can proceed indefinitely without interruptions, resulting in increased product throughput.

The r- $\theta$ -z robot approach (option C) is a commonly used method for wafer handling in the semiconductor processing industry. In that industry, speed is a secondary consideration to cleanliness (minimum particulate generation) and sometimes other special factors, such as vacuum compatibility. These robots are highly flexible and programmable in their range of motion. For example, the Cybeq r- $\theta$ -z robot could be an elegant cell loading system, since it eliminates all other loading process mechanisms (elevator and shuttle mechanisms). Its flexibility in motion exacts a price in throughput, however, since nearly all of its motions must be done in series. As shown in Table III, the process required to load a cell requires 11 separate motions calculated to take 4.2 seconds per cell, using the robot's *maximum* speeds in all three axes and allowing one second for picking a cell from the top of a stack. Five to six seconds is a more realistic estimate for the cycle time, given that each motion requires an acceleration up to the maximum speed and a deceleration to rest. Thus each motion cannot run at maximum speed through the full range of motion. Since this cycle time is too slow to meet our four second per cell throughput goal, the r- $\theta$ -z robot approach has been eliminated from consideration.

Options A, B, and D are all potentially faster than option C since the cell stack vertical motion is done concurrently with the cell pick-and-place operation. A version of option D is commercially available from AMI. This system, called a dual stack magazine loader, is typically used to load ceramic substrates into screen printers for hybrid circuit or surface mount applications. It includes an air pad pick-up that uses the Bernoulli effect to pick up the top cell from a stack. AMI loaned an air pad to Spire which was then evaluated with stacks of thin cells. These tests at Spire showed that the Bernoulli pick up will probably work with thin cells, although the unit consumes a large amount of compressed air.

The AMI throughput rating of 1200 parts per hour (3 s/cell) is probably not achievable with thin cells, but it should be able to meet the four seconds per cell requirement. However, the largest cell size which the standard system can handle is 11.4 cm (4.5-inch) square, smaller than our requirement of 15 cm (6-inch) square. As a result, the AMI system is not acceptable.

**Table III** *Cell loading with r- $\theta$ -z robot running at maximum rated speeds.*

Step	Description	Time (s)	Comments
1	Move down 9 cm (3.5"), z	0.25	Average distance for 18 cm (7") stack
2	Pick up cell with vacuum	1.00	
3	Move up 9 cm (3.5"), z	0.25	Average distance
4	Move in 16 cm (6.5"), r, during up motion	0.29	Maximum cell size plus clearance: 0.54s total
5	Rotate 90°, $\theta$	0.28	
6	Move out 16 cm (6.5"), r	0.54	Position cell over aligner
7	Move down 0.6 cm (0.25"), z, and release cell	0.60	Place cell on aligner
8	Move up 0.6 cm (0.25"), z	0.10	
9	Move in 9 cm (3.5"), r	0.29	For 7.6 cm (3") end effector
10	Rotate 90°, $\theta$	0.28	
11	Move out 9 cm (3.5"), r	0.29	
Total at maximum rated speeds		4.19	$r_{\max} = 30$ cm/s, $\theta_{\max} = 320^\circ$ /s, $z_{\max} = 35$ cm/s
Estimated total at realistic speeds		5.0 to 6.0	

The stack loader which Spire designed and builds for its SPI-TAB™ 1000 tabbing machine was also evaluated for use in this program. The loader has a single elevator with multiple shelves for cell stacks and an optical sensor to maintain the proper stack height. A rotary pick-and-place arm ( $\theta$  and z motions) with vacuum cups picks up cells from the top of the stack. A compressed air jet and a cell flexer (which slightly bends the top cell as it is being picked up) are used to separate the top cell from those under it in the stack, since quickly picking up a cell creates a temporary low pressure region under the cell which tends to lift additional cells in the stack, especially if they are thin.

While this loader works well and has a number of good features (the optical stack height sensors, the air jet, and the cell flexer), it has not been selected for use in its present form because two aspects can be improved to maximize throughput. Firstly, the present system has no stack shuttle, which requires that the machine be interrupted for inserting cell stacks into the elevator. Secondly, the air driven rotary pick-and-place arm has a tendency to bounce at the end of travel when operating at high speeds.

Since no system has been found which satisfies all the requirements for this application, Spire designed a custom system for loading cells. Option A (in Figure 6) was selected over option B because the linear stack shuttle is a simpler mechanism than the rotary shuttle. A layout drawing of the cell loading system is provided in Figure 7. The drawing also shows the cell aligner system, which is mounted on the same frame.

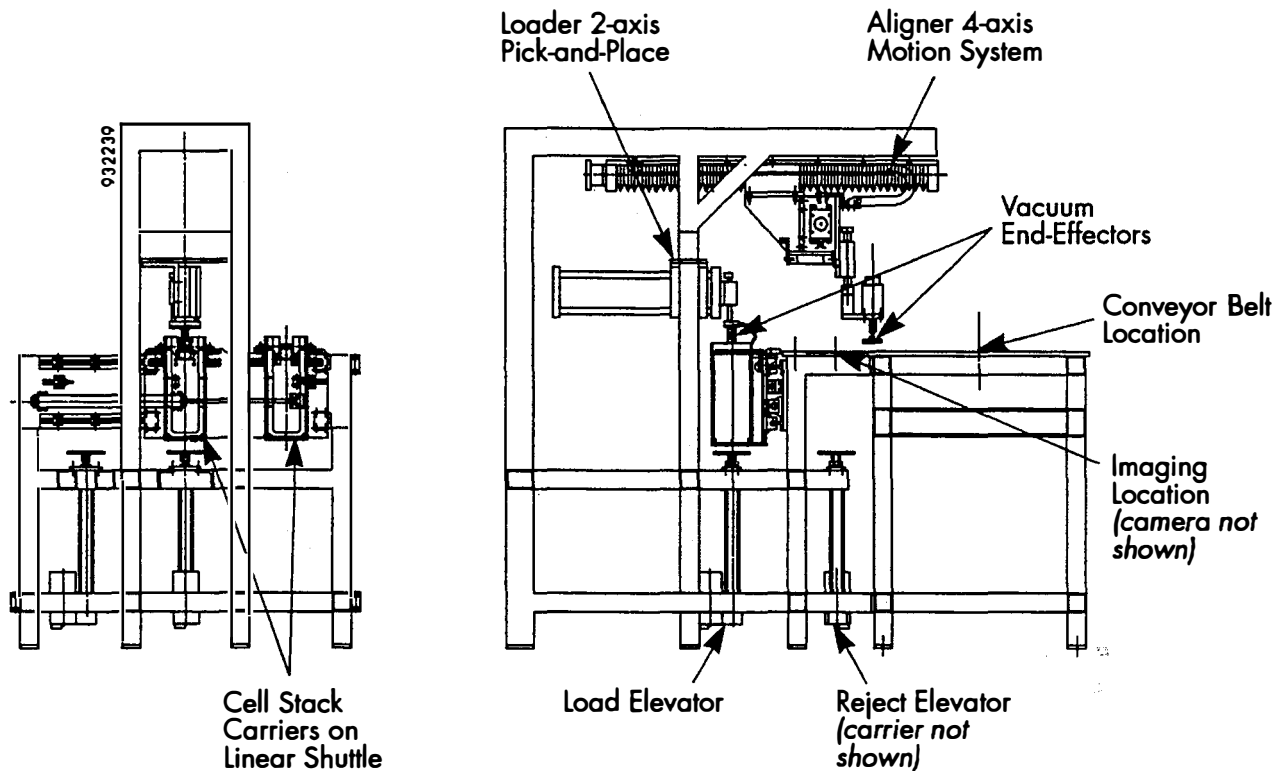


**Figure 7** *Lay-out of the cell loading and alignment systems.*

All of the loading system components have been designed, fabricated, and installed in the frame. A photograph of the loading and aligning systems is provided in Figure 8.

The cell pick-and-place mechanism uses air actuated linear slides with ball bushing mounts for moving the cell in x and z axes. Hydraulic cushions allow higher speed operation by reducing end-of-stroke vibrations. A vacuum pick-up end-effector with a mechanically floating mount was designed to minimize stress on thin cells during pick up and placement. A flexible bushing is used for compliance in potential out-of-plane conditions between the cell stack and the end effector. Vacuum is provided to the end effector by a vacuum aspirator assembly, which includes a venturi vacuum pump, a filter, a vacuum switch to indicate the presence of a cell, and a vacuum breaking valve for rapid and positive release of the cell.

Quick-release stack carriers were designed for holding cell stacks on the shuttle mechanism and at the reject elevator. Each carrier has the capacity to hold a stack up to 25 cm high, equivalent to 1000 cells with a thickness of 250  $\mu\text{m}$  per cell. At a processing rate of 4.0 s/cell, a full stack will take 66.7 minutes to unload.

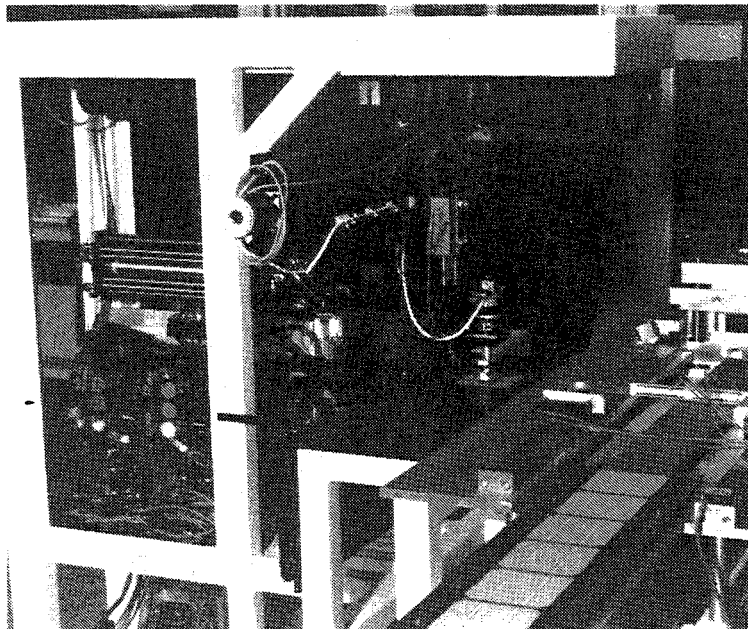


**Figure 8** *Cell loading and aligning systems.*

The stack shuttle is mounted on linear ball bushings and driven by an air cylinder. The shuttle transports two stack carriers back and forth between the load elevator and locations on either side of the elevator for removing empty carriers and inserting full ones.

The load and reject elevators are driven by linear electric cylinders (lead screw type) controlled by optical sensors. As cells are withdrawn from a stack by the pick-and-place mechanism, a sensor directs the load elevator to raise the stack, thus maintaining the top of the stack at the proper height. Similarly, as cells are placed in the reject carrier, a sensor signals the reject elevator to lower the stack, maintaining the top of the reject stack at the proper level. Additional sensors detect when a carrier on the load elevator is empty and when a carrier on the reject elevator is nearly full.

Air jets were designed to separate the top cell from the others in the stack. The jets direct streams of compressed air at opposite sides of the cell stack to fill the low pressure region created under the cell by the pick-up operation. The effectiveness of the air jets will be tested in 1994.

Position sensors are installed on all mechanisms (cell pick-and-place, stack shuttle, and elevators) to prevent collisions. The sensors also increase processing speeds, since they can signal the process controller to execute the next step in a sequence as soon as conditions are safe.

### 2.2.3 Task 3 - Cell Alignment Process Development

Spire engineers are working with a team from the University of Massachusetts Lowell (UML) Center for Productivity Enhancement to develop the cell alignment process subsystem. Spire has taken the lead in the mechanical design aspects, such as the design of the structural frame, the cell manipulator, the aligner stage, and the various mounting brackets. UML is developing the vision system, including the camera, lighting, imaging board, and software, as well as the control software for the 4-axis aligner manipulator and the 2-axis cell loader manipulator.

Discussions between Spire and UML early in the program resulted in the development of an alignment process algorithm. The process steps are listed in Table IV.

**Table IV** *Alignment process steps. Motion directions are in parentheses.*

Step	Description
1	Acquire cell image
2	Process image to locate and inspect cell
3	Move vacuum end effector to cell center (x, y)
4	Pick up cell (z)
5	Align and transport cell to conveyor belt or reject elevator (x, y, $\theta$ )
6	Place cell on conveyor or reject elevator (z)
7	Return vacuum end effector to home (x, y, $\theta$ )

The ease with which an optical pattern recognition system can discriminate between a cell's metal grid pattern and the un-metallized silicon can be demonstrated with a very simple test: making a Xerox copy image of a cell. A photocopy of a Solec cell is provided in Figure 9 as an example. The test shows that with the proper lighting a very high contrast image can be recorded. This contrast is a natural outcome of the need to absorb sunlight between the grid lines (which leads manufacturers to incorporate anti-reflection coatings and/or texturized light-trapping surfaces) and the reflective properties and smooth surfaces of the contact metal. High contrast will make it easy to grab a two dimensional bit map image of the cell where pixels are either on, due to contact reflection, or off, due to silicon absorption.

Essentially all terrestrial one-sun silicon cells have contact patterns that contain two linear and parallel bus regions connected by narrower grid lines. A mathematical algorithm for aligning such patterns has been conceived that rapidly computes the center of a cell's contact pattern and the pattern's angular position. In general, this is the only information needed to align the cell. A vacuum pick-up end effector mounted on a four axis motion control system moves in x-y to the center of the pattern, picks up the cell, and simultaneously rotates the cell while moving it in x-y to place it in the proper position on the cell string conveyor.

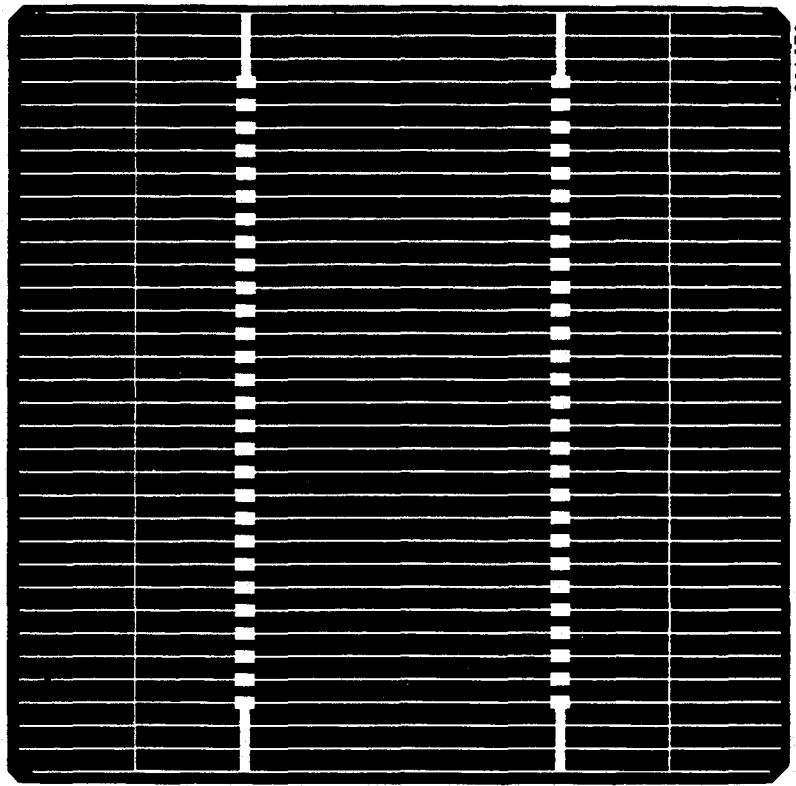


**Figure 9** *Xerox copy image of a Solec cell.*

A four axis ( $x$ - $y$ - $z$ - $\theta$ ) motion system for aligning and transporting cells was selected and custom fabricated by a vendor to meet our specifications. The system is installed in the frame used for the loader, as shown in Figure 8, previously. Position sensors allow homing, end of travel, and collision prevention functions, through software control. A vacuum pick-up end effector was fabricated with the same design as the one used to pick up cells from the load elevator, except that the flexible coupling was replaced with a rigid coupling to improve the alignment accuracy.

The aligner stage is located centrally between the reject elevator ( $y$  direction) and the cell string conveyor ( $x$  direction). This design reduces the amount of travel time needed to move the cell from the aligner to the conveyor and return the end effector.  $X$  and  $y$  motions are stepper motor driven lead screw assemblies,  $z$  is air actuated, and  $\theta$  is stepper motor driven. The stepper for  $\theta$  has  $0.18^\circ$  resolution (2000 counts per revolution) which is expected to be sufficiently accurate. If testing indicates that greater accuracy is needed, 10:1 and 18:1 ball reducers are available. Open frame controllers, which communicate via an RS232 port, have been selected for the three stepper motors ( $x$ ,  $y$ , and  $\theta$ ) instead of more expensive fully packaged controllers with control panels.

In operation, the loading system places a cell face down on the aligner stage, a glass plate with a frame which limits the distance that the cell can slide after placement. A camera and a lamp are mounted underneath the stage, looking upwards to obtain an image of the cell's front contact. A video board captures the image for analysis. The cell is located in  $x$ ,  $y$ , and  $\theta$ , and inspected for defects, such as breaks, chips, unrecognizable grid patterns, or upside-down placement. Rejected cells are placed in the reject stack carrier, while good cells are placed in the proper location on the conveyor belt.

The video camera, lighting system, and software are now under test. While images of cell contact patterns can be obtained, problems have been encountered in detecting the cell edges. This problem is caused by the optically noisy ambient background above the cell. Experiments with lighting and white backgrounds will be done in early 1994.

#### 2.2.4 Task 4 - Interconnect Ribbon Handling Process Development

The mechanical design of processing subassemblies for ribbon handling, bending, and cutting has been completed. A drawing which labels the important components of the ribbon handling system is provided in Figure 10. These components are the ribbon reel assembly, the flux station (which includes the ribbon drive assembly), the ribbon accumulator, the ribbon clamp and form assembly, the ribbon cutter, and the ribbon shuttle assembly.

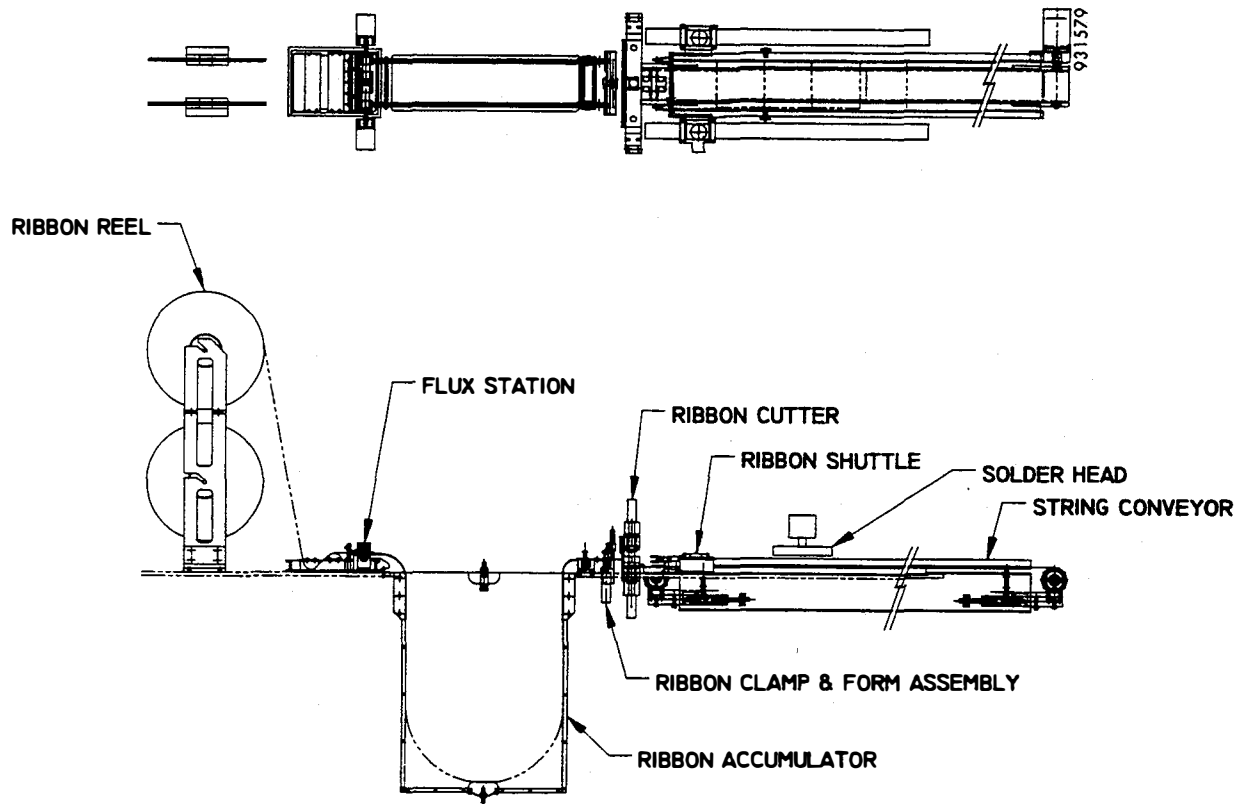


**Figure 10** *Components of the ribbon and cell handling system.*

As part of the initial design work, a story board was created in CAD to illustrate the sequence of events needed to produce a string of soldered solar cells. The story board was a valuable aid in the mechanical design of the ribbon handling system, as it facilitated the design of mechanisms capable of executing all of the processes needed to produce cell strings, and of executing them in the proper sequence. The process sequence is as follows:

- The ribbon shuttle, a pair of air actuated mechanical grippers mounted on linear motors, pulls two interconnect ribbons a distance at which a stress-relief bend is formed in each ribbon. The ribbons are pulled again to a position at which they are cut (cut ribbons are referred to as tabs). The tabs are then pulled to place them in the desired location for assembly. Linear motors were selected to provide rapid, precise, and programmable positioning of the ribbon.
- A vacuum conveyor belt holds the left ends of the tabs while the grippers open and retract to the right, dropping the tabs' right ends onto the belt. The grippers then move left to acquire the ribbons for the next pair of tabs; at this time a cell is placed by the aligner in the first cell position, on top of the first set of tabs. The ribbon forming, cutting, and placing process is repeated, with the right half of the second pair of tabs placed over the first cell, and the left half placed on the vacuum belt. The vacuum conveyor indexes the cell and tabs the length of one cell plus the gap between cells.
- The tab fabrication, cell placement, tab placement, and cell indexing processes are repeated as needed to build up a string of any desired length. When a cell is in its third location on the vacuum conveyor it is soldered to both the top and bottom tabs in one step. After the last cell in the string is soldered, the conveyor indexes the string to the proper location on the belt for removal with the string transfer assembly.

Solder coated copper ribbon material is typically supplied as a coil wound on a cardboard reel. The ribbon reel assembly design was modified from that used in Spire's tabbing machine to increase the reel diameter capacity from 30 cm (12-inch) to 38 cm (15-inch). This increase lengthens the interval between reel changes by approximately a factor of two. The interval is a function of reel diameter, machine throughput (seconds per cell), cell size (length of ribbon across the front and back of the cell), spacing between cells, and ribbon thickness (since more thin ribbon will fit on a given diameter reel). For example, assuming a 4 s/cell throughput, 102 mm cells, 2 mm spacing, 75  $\mu\text{m}$  thick copper ribbon, and 12  $\mu\text{m}$  thick solder plating, a 30 cm diameter reel will last approximately two hours and ten minutes, while a 38 cm diameter reel will last approximately four hours and twenty minutes.

The ribbon reel assemblies, shown in Figure 11, were designed in May and fabricated and assembled in July. Each of the two reel assemblies (left and right) supports two stock reels (upper and lower) to allow ribbon splicing from the trailing end of ribbon from an empty reel to the leading end of ribbon from a full reel. While the splicing operation will be manual, it eliminates the time consuming manual threading operation which would otherwise be required whenever a reel empties. Referring to Figure 10, the operation would require threading ribbon through the flux bath, drive rollers, accumulator, clamp and form assembly, and ribbon cutter.

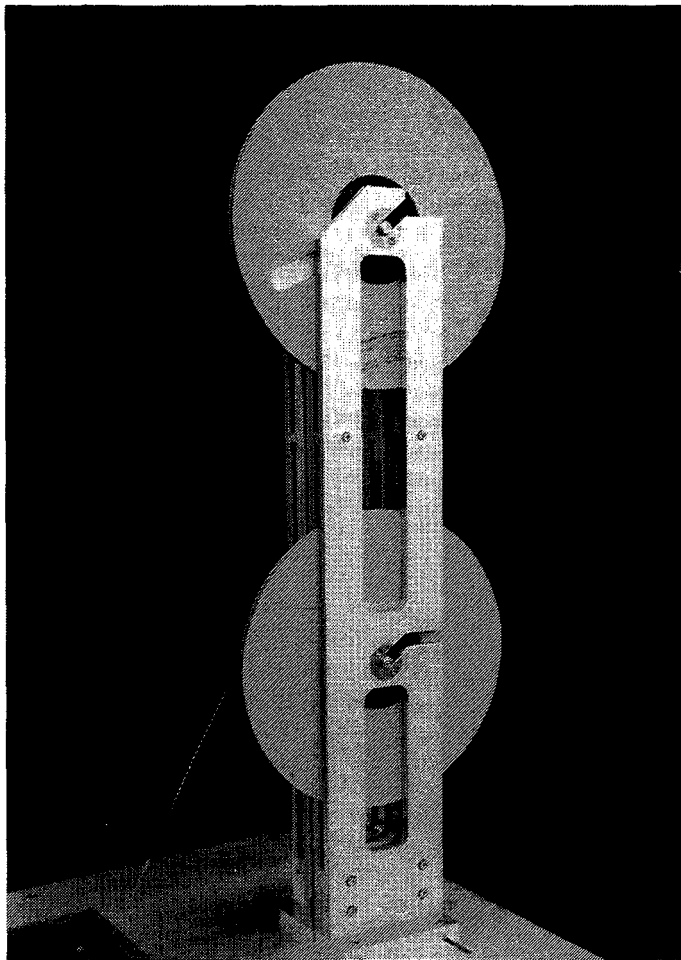


**Figure 11** *Photograph of the ribbon reel assembly.*

The ribbon accumulator assembly design was completed in May and the components were fabricated and assembled in June. A layout drawing is provided in Figure 12. As with the ribbon reel assemblies, both a left and a right version were designed. Part of the two accumulators are shown in the foreground of Figure 13. A similar accumulator is used in Spire's SPI-TAB™ 1000 tabbing machine to allow rapid feeding of ribbon onto the cells without rapid rotation of the stock reels. This new version of the accumulator has been lengthened and widened to store more ribbon. The ribbon shuttle can draw upon this ribbon supply for a short period of time while the operator splices ribbon from a new reel. If the operator is available to make a splice before the accumulator is emptied the machine can continue without interruption.

Four ribbon sensors are used, two on each accumulator. An optical sensor is located at the bottom of each ribbon loop to turn off the ribbon drive motor (at the flux station) when the accumulator is full. A metal proximity sensor at the top of each accumulator (one is visible in Figure 13) signals the ribbon shuttle to stop extracting ribbon if either accumulator is empty, a situation that may occur, for example, if the operator is unavailable to splice in a new reel of ribbon. In addition, optical sensors have been selected for indicating when a reel has run out of ribbon. Two sensors, one for each ribbon path, will be mounted between the flux station and the ribbon reels. When a reel empties, the sensor will signal the ribbon drive motor to stop feeding ribbon into the accumulator and signal the operator to splice in a new reel.

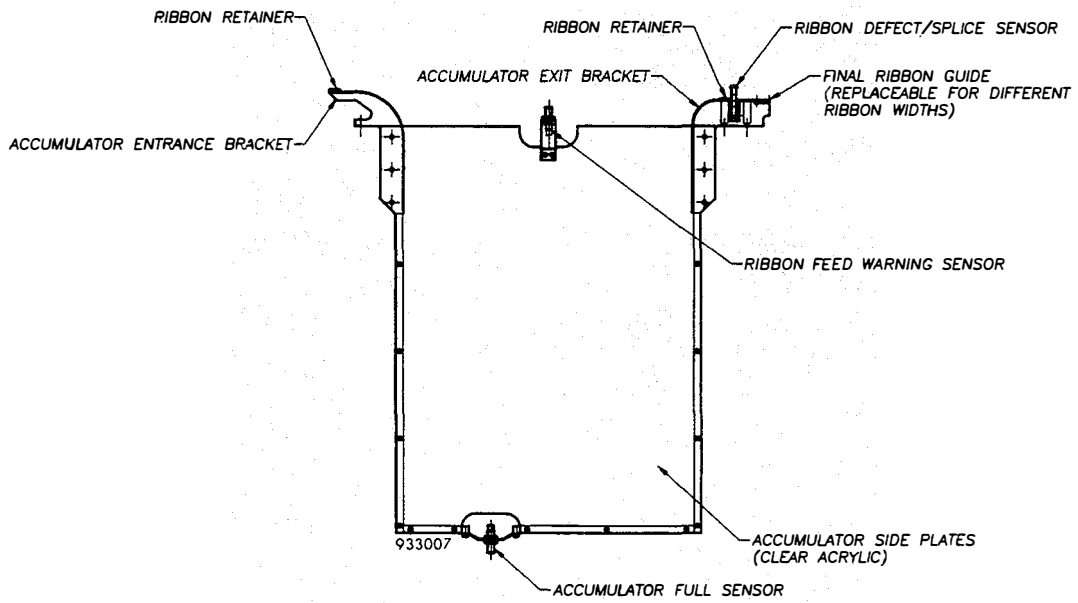


**Figure 12** *Ribbon accumulator assembly lay-out drawing.*

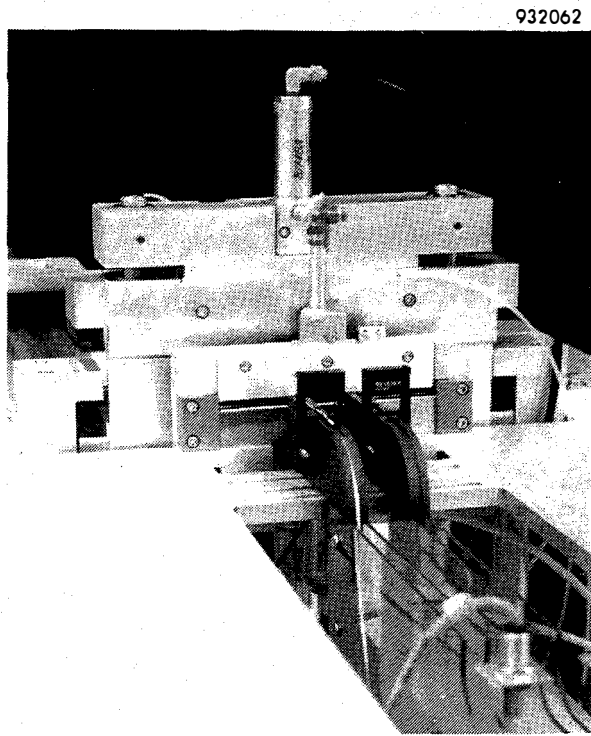


**Figure 13** *Photograph of part of the interconnect handling system. From foreground to background: the accumulators, the splice sensors, the clamp and form assembly, and the ribbon cutter.*

An additional, more sophisticated optical sensor has been selected for sensing the presence of a splice. Two of these sensors are mounted at the exits of the accumulators in Figure 13. They direct the ribbon handling system to automatically cut off the spliced section and deposit it in a "trash bin." These sensors will also be useful in detecting defects such as kinks in the ribbon material. The sensors were bench tested at Spire in the following manner. A hand-soldered ribbon splice was made by overlapping two solder coated interconnect ribbons and heating them with a soldering iron. No flux was used since there is solder on both parts. The spliced ribbon was pulled through the sensor several times and the splice was reliably detected.

The ribbon clamp and form subassembly, also seen in Figure 13, was designed and fabricated in April. A lay-out drawing is provided in Figure 14. The ribbon forming section produces a stress-relief bend in the two interconnect ribbons. A metal die machined with the shape to be transferred to the ribbon is driven upwards by an air cylinder against an elastomeric pad. Initially designed with a urethane pad, ribbon forming tests showed that the ribbons were not obtaining the full die shape, an indication that the urethane pad is too hard. The pad was replaced with a length of lower durometer fluoroelastomer O-ring material seated in a captive groove. Testing showed that the O-ring material transfers the metal die shape to the ribbon very well. The groove design makes maintenance or replacement of the elastomer trivial.

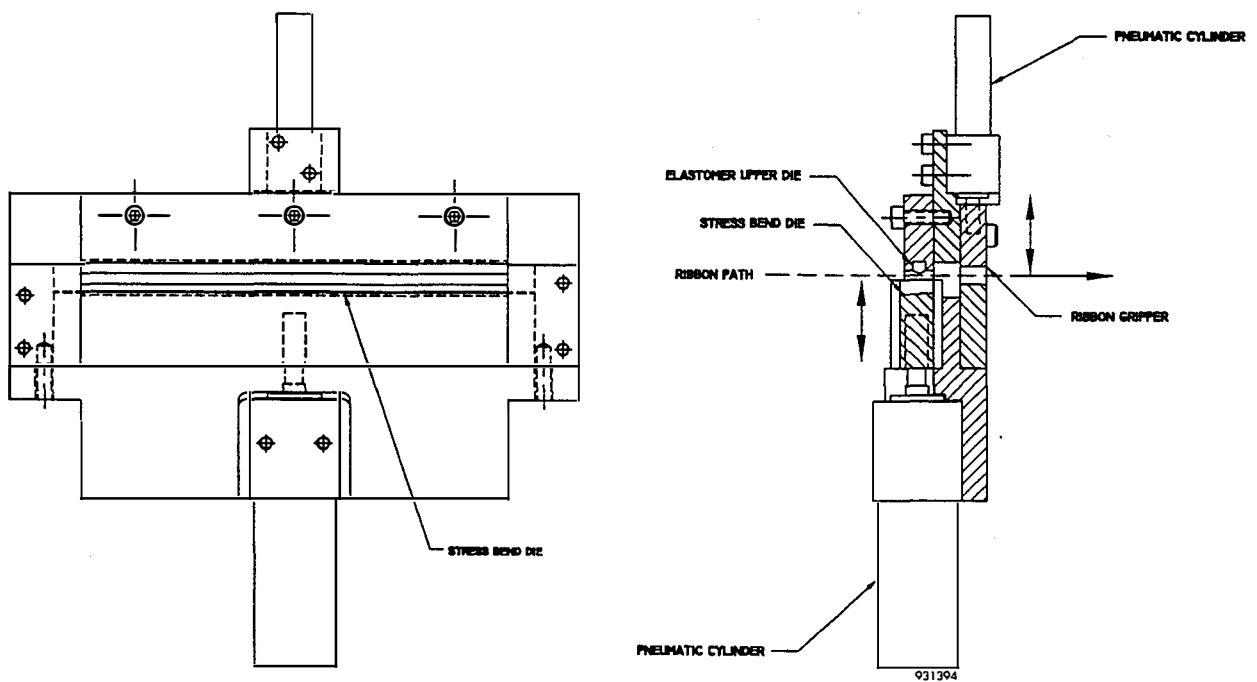


**Figure 14** *Ribbon clamp and form assembly.*

The clamp section of the clamp and form subassembly holds the two interconnect ribbons while they are being cut to prevent them from falling under their own weight into the accumulator. The small air cylinder on top of the clamp and form subassembly (Figure 14) actuates the clamp.

The ribbon cutter assembly is used to cut the two interconnect ribbons to the desired length. The initial concept had two sets of cutting blades (one set for each ribbon) mounted on horizontal slides so they could retract away from the path of the grippers on the ribbon shuttle assembly. The concept was modified in the final design to eliminate the horizontal motion by using a single large blade set for both ribbons, thereby simplifying the mechanism and increasing its speed. Both blades move vertically away from the ribbon after cutting to provide clearance for the ribbon shuttle. The upper and lower blades are mounted on ball bushings and are driven by air cylinders. The assembly is shown in Figure 15 and in the background of Figure 13.

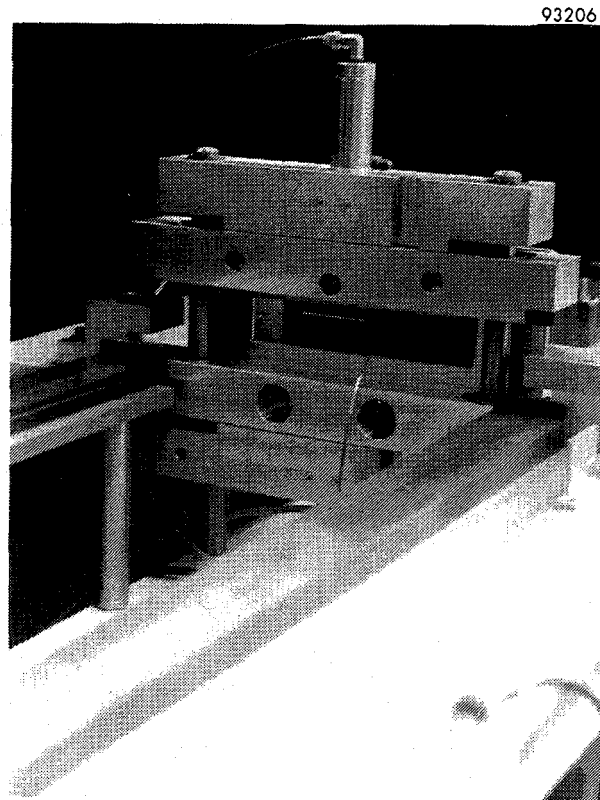


**Figure 15** *Ribbon cutter assembly with blades in the open position.*

The ribbon cutter assembly was designed in April and the components were fabricated and assembled in May. The blades were honed and the air cylinders were installed in June. Bench tests were successful in reliably cutting solder plated copper interconnect ribbon.

The ribbon shuttle assembly uses a pair of programmable linear stepper motors to move end effectors that grip the two interconnect ribbons, thereby determining the stress-relief bend position, the tab length, and the tab placement position. The end effectors are suspended over a conveyor belt on which the tabs and cells are placed for assembly. The motors must work in tandem while being connected mechanically, without racking problems. A vendor of linear motors visited Spire in April to test such mechanically-linked tandem operation prior to committing to this design. Spire fabricated an aluminum plate which was securely bolted to two forcers (moving stages) on two platens (the fixed part of the motor). The motors were then driven through a simulated interconnect feeding cycle at reasonably high speeds, comparable to

the speeds we will be required to run in production. No racking, binding, or other problems were observed. Based on the positive results of these tests, a detailed design was completed for the ribbon shuttle assembly, which includes the linear motors, end effectors for gripping the ribbons, position sensors for homing and end of travel, and structural elements.

Components for the ribbon shuttle assembly were ordered and fabricated in May. A specially designed mounting bracket was fabricated for attaching the two air actuated ribbon grippers to the linear motors. The grippers have integral position sensors that indicate whether they are open or closed. The linear motors, drivers, and controllers were delivered to Spire and installed in July. A photograph of the shuttle assembly is provided in Figure 16.

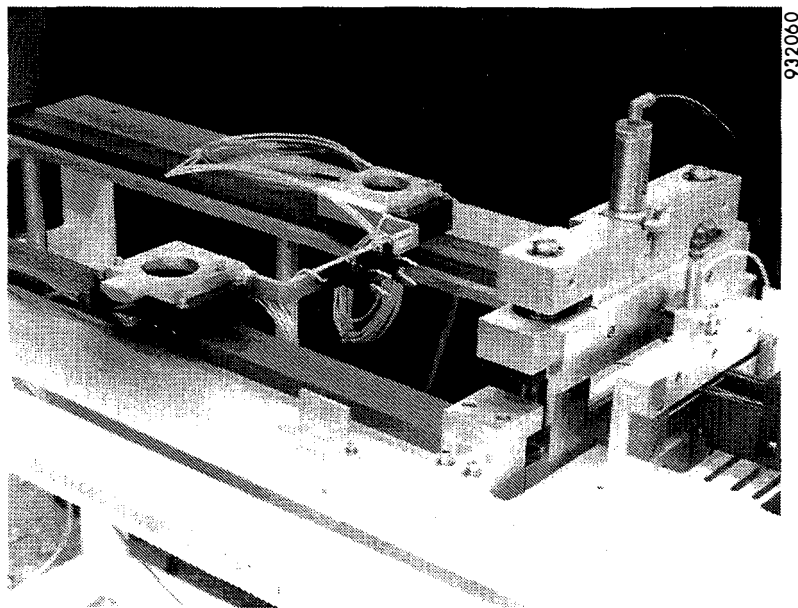


**Figure 16** *Ribbon shuttle assembly with grippers open.*

### 2.2.5 Task 5 - Solder Flux Application Process Development

Two alternative approaches were considered for automatically dispensing solder flux or solder paste to the solder joints: a syringe dispenser method and a ribbon coating method. In the first approach, a pair of syringes would be located over each interconnect tab and actuated in x and z to dispense a pair of lines of flux or paste onto the tabs. A cell would then be placed face down on the flux/paste coated tabs and the operation would be repeated on the rear surface of the cell before the next set of tabs is placed over the cell.

Spire engineers visited Camelot Systems in Haverhill, MA, on April 2, to investigate the feasibility of the syringe dispensing approach. Camelot manufactures automated solder paste, flux, and adhesive dispensing equipment used for hybrid circuit and surface mount applications. The equipment is good quality, has more than adequate precision, and is very flexible in terms of its motion control programmability. Unfortunately, it cannot be operated fast enough to meet our requirements. If the syringes were driven at the speeds needed to obtain sufficient throughput for this application (4 s/cell), they would not be able to dispense continuous lines, due to the surface tension and viscosity of the paste or flux.

The use of a greater number of syringes (*e.g.*, six per tab) to simultaneously dispense multiple dots of paste or flux should be capable of meeting the throughput requirement. Unfortunately, this approach can only dispense discrete dots, not continuous lines of flux or paste. In addition, the large number of dispenser controls required for this approach makes it mechanically complex.

The ribbon flux coating process has a number of advantages over syringe dispensing: it requires minimal mechanism, it adds no time to the assembly process, and it coats the entire ribbon with flux. Therefore, ribbon coating was selected for development. In this process, the ribbon is pulled through a flux bath as it is being fed from the stock reels by a drive roller. In principle, this is a very simple method since ribbon must be fed from reels regardless of whether flux is applied or not. However, sufficient flux must be applied to the interconnect ribbon for reliable soldering without generating unacceptable flux residues on the cells or on the ribbon feed system components.

Components for a prototype interconnect ribbon fluxing subassembly were designed, fabricated, and assembled. A photograph of the assembly and a reel of interconnect ribbon used for preliminary flux coating tests is shown in Figure 17.

The flux used for these tests was Multicore Xersin<sup>®</sup> 2112, a low solids content, non-corrosive, no-clean flux. Solder plated copper ribbon was pulled from a reel through a flux bath by motor-driven urethane coated rollers. Two large-radius cylinders with D-shaped cross-sections diverted the ribbon through the flux. A squeegee type wiper was used to limit the quantity of flux on the ribbon.

Samples of flux coated ribbon were soldered to a solar cell with a soldering iron without additional flux or solder. The ribbons were then destructively peeled from the cell to examine the solder joint area. A small amount of soldering occurred at one edge of the ribbon, but most of the flux was wiped off of the ribbon surface. This indicates that the squeegee removed too much flux to make adequate solder joints.

The test was then repeated using the same procedure as described above but without the use of the squeegees. In this case, excellent solder joints were produced. The solder joint areas covered nearly the full area under the interconnect ribbons and the joints were strong enough to pull silicon out of the wafer. Both the top and bottom surfaces of the ribbon soldered equally well.

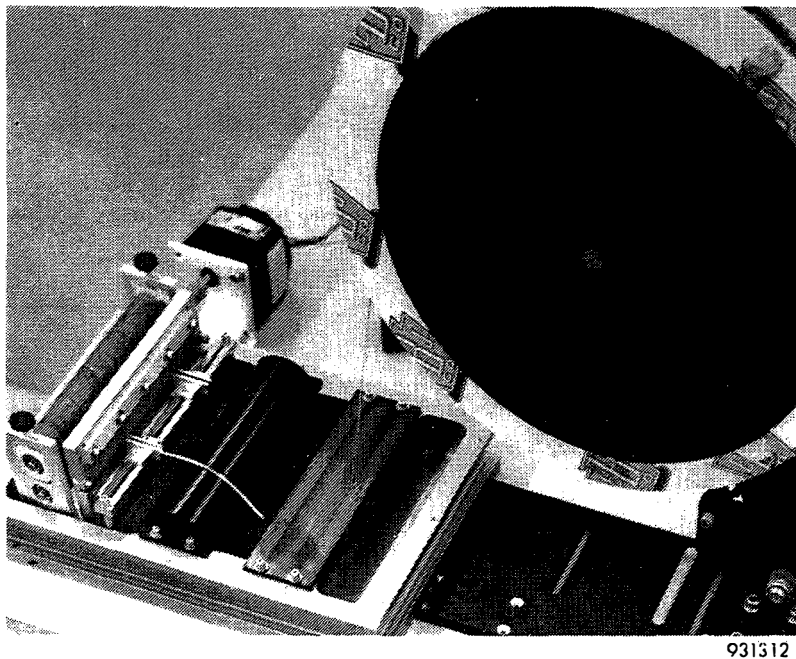


**Figure 17** *Prototype ribbon flux coating subassembly with interconnect ribbon reel.*

Further testing with the prototype system revealed a problem with the ribbon drive rollers. Without the squeegee, large amounts of wet flux accumulated on the urethane drive rollers, and the ribbon intermittently stuck to the roller and wrapped around it. New rollers were fabricated from DuPont Teflon® to see if a smoother, lower friction roller material would help solve the problem. At the same time, the assembly was modified to add a second set of rollers and a second motor, to provide independent feeding for two interconnect ribbons.

Tests with the Teflon roller showed that the sticking problem is not caused by the roller material but by the flux. During continuous operation, the ribbon fed properly. However, when the rollers sat idle long enough for the flux to dry, the ribbon occasionally stuck to the rollers and wound around them, due to the tackiness of the dried flux on the rollers. This was observed with both the urethane and the Teflon rollers.

Several strategies for solving the flux sticking problem were then investigated: air jets were added to dry the flux on the ribbon; the 2112 flux was thinned to reduce the solids content; and two additional flux types were evaluated. The air dryers, mounted between the flux bath and the ribbon drive rollers, consist of two pairs of air jets, one jet above and one below each ribbon, connected to a source of pressure regulated compressed air. After installing the air jets, three kinds of non-corrosive fluxes and two kinds of flux thinners were tested in the flux station. A summary of the test results is presented in Table V.

The first flux tested was Multicore 2112, the same flux used prior to the flux station modifications. The air dryers were found to be highly effective in reducing the amount of flux on the ribbon as it enters the rollers, but they did not completely eliminate the problem of the ribbon sticking to the rollers. Flux thinner recommended for use with the 2112 was obtained and mixed with the flux in a 1/1 ratio by volume, decreasing the solids content from 12% to 6%. Ribbon feeding tests were repeated but the ribbons still occasionally stuck to the rollers.

**Table V** Flux testing summary.

Flux Type	Solids Content	Solvents	Sticks Ribbon to Rollers	Solderability to Solec Cells
Multicore 2112	12%	Alcohols & ketones	Yes	Fair
Multicore 2112	6%	Alcohols & ketones	Yes	Fair
Multicore X32-10M	2%	Propanol & methanol	No	Poor
Kester 2331	14%	Propanol & glycerol	No	Good
Kester 2331	2%	Propanol & glycerol	No	Good

The second type of flux tested was Multicore X32-10M, a halide-free no residue flux with the look and smell of pure alcohol (propanol and methanol blend). The drive rollers had no problems processing ribbon with this flux coating. No sticking or ribbon wind-up was observed. Unfortunately, this flux was not effective in soldering ribbons to Solec cells, either by light soldering or by hand, with a soldering iron.

The third flux tested was Kester 2331, a neutral pH organic flux. The flux was tested both at full strength and thinned to a 1/6 ratio by volume, decreasing the solids content from 14% to 2%. This flux presented no problems for the ribbon handling system, including the drive rollers. In addition, excellent solder joints were made to the Solec cells with this flux, both manually (soldering iron) and automatically (light soldering). This flux was then used in the solder process development work described in Section 2.2.6, below.

The ribbon flux coating assembly in its present form is shown in the lay-out drawing in Figure 18 and the photograph in Figure 19. The assembly contains a float switch and a peristaltic pump for automatically maintaining the proper flux level. A cover with a vent tube has been added to trap and exhaust solvent fumes. The ribbons travel around a pair of diverters to immerse them in flux, through the air dryers, and through a pair of adjustable ribbon guides that provide alignment for the ribbon as it enters the drive rollers.

#### 2.2.6 Task 6 - Ribbon to Cell Solder Process Development

Spire is incorporating its light soldering technology for use in this program. A pair of high intensity lamps that emit over a broad spectrum (visible and infrared) provide radiant energy to solder the interconnect ribbons to the solar cells. This light soldering process was developed at Spire to replace conduction soldering, in which heated elements physically contact the ribbons to make discrete solder joints. Light soldering allows continuous solder joints to be made while generating less mechanical and thermal stress, since no direct contact is made to the cell or ribbons for heat transfer. In addition, light soldering greatly reduces maintenance, since it eliminates the frequent cleaning required for the heated elements used in conduction soldering. These elements quickly pick up a layer of molten solder from the ribbon which then oxidizes on the hot elements. Frequent cleaning is required since the oxide is insulating and interferes with good heat transfer.

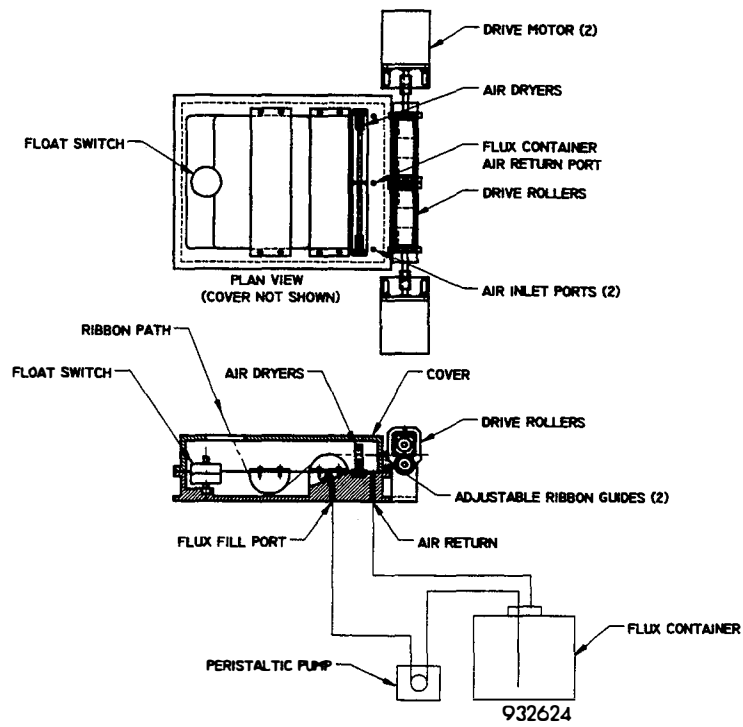


**Figure 18** *Lay-out drawing of the flux station assembly.*

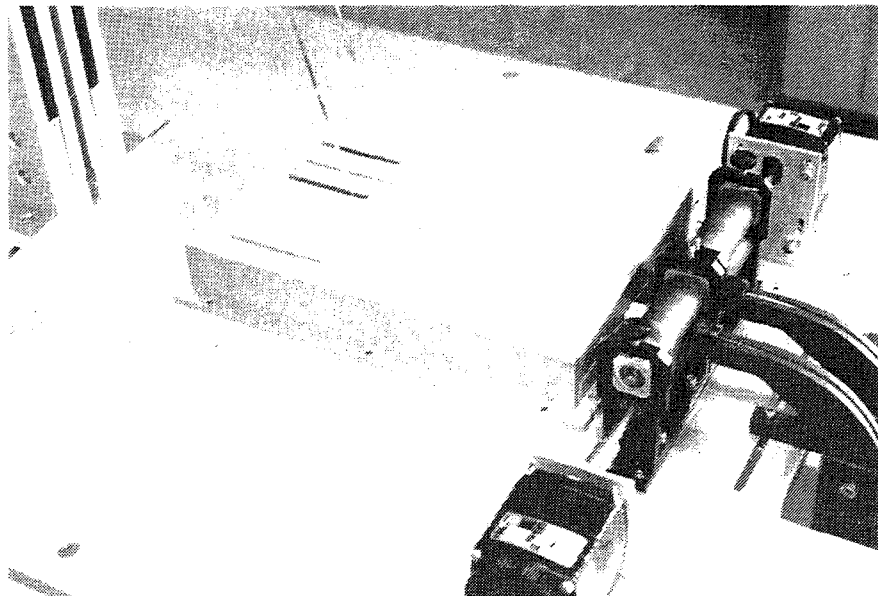


**Figure 19** *Photograph of the flux coating subassembly.*

Light soldering processes are used in Spire's existing cell tabbing and connecting equipment (the SPI-TAB™ 500, the SPI-TAB™ 1000, and the SPI-CONNECT™ 1000) for soldering tabs to either front contacts or back contacts. In this program, a new process is being developed for soldering to both the front and back surfaces of thin cells simultaneously, thus reducing the number of heating steps used for soldering from two to one. In addition, conduction pre-heating of cells is being used with light soldering for the first time to reduce thermal stress during soldering and to increase throughput.

Components for the two lamp solder head assembly were fabricated and assembled as shown in the lay-out drawing provided in Figure 20. The assembly includes two high power lamps, air cooling for the lamp seals, protective windows and flux vapor exhausts to keep the lamps clean, and low force springs to hold the tabs in contact with the cell during soldering. The lamp mounts are slotted to allow the lamp spacing to be adjusted to match the tab spacing. The solder head assembly can be easily disconnected from the actuator assembly for ease of servicing.

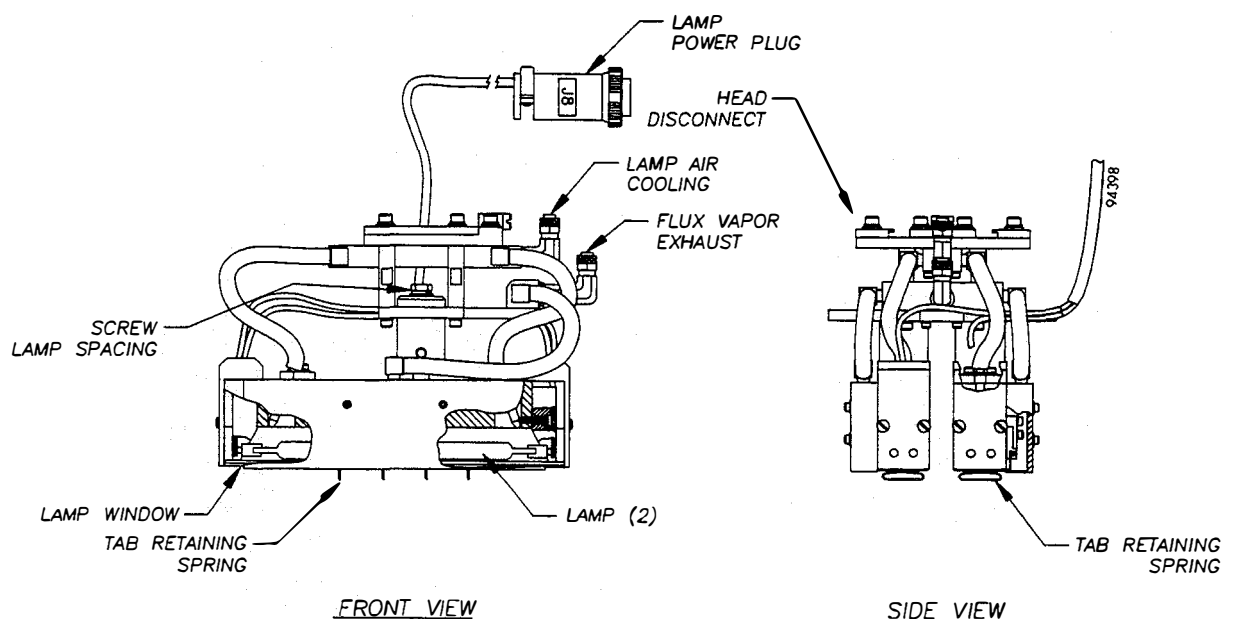


**Figure 20** Two lamp solder head assembly.

The solder head actuator assembly moves the solder head up and down during soldering. When the solder head is down, the tab retaining springs lightly press the interconnect tabs onto the cell contacts until the solder freezes. Components for the actuator assembly, shown in Figure 21, were fabricated and assembled. The lamp assembly attaches to the mounting plate at the bottom of the actuator assembly. A ball slide provides smooth vertical motion which is driven by an air cylinder. Air flow control valves regulate the solder head speed, while magnetic reed switches indicate the head position.

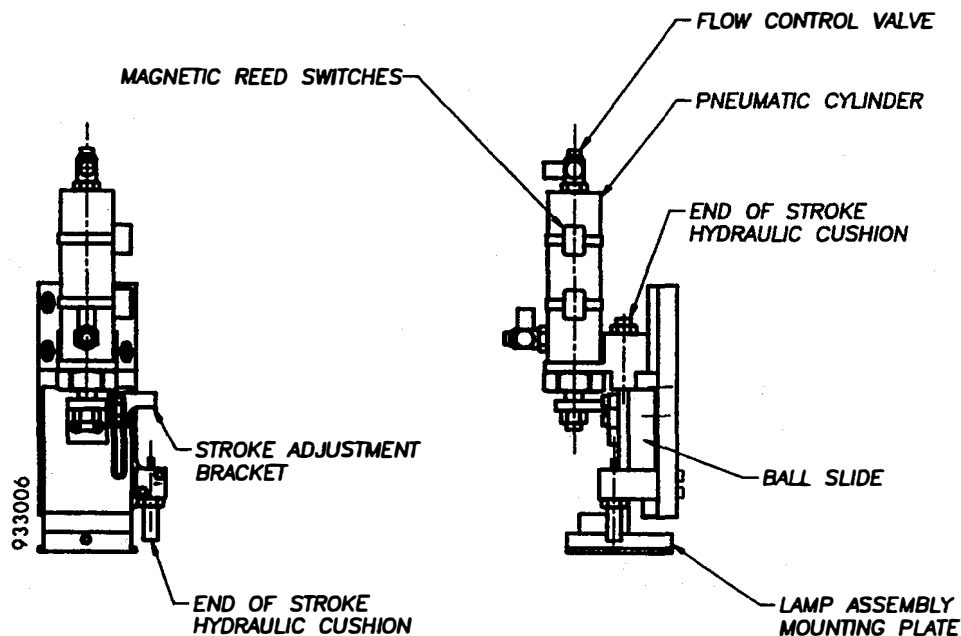


**Figure 21** *Solder head actuator assembly.*

Special components were designed and fabricated for mounting the solder head over the vacuum conveyor belt. The solder head, actuator, and mounting hardware have been assembled and installed, as shown in the photograph in Figure 22.

Solar cell soldering tests began in November. Pairs of solder coated copper interconnect ribbons were automatically flux coated, formed with a stress-relief bend, cut to length, and placed on the vacuum conveyor belt for assembly with solar cells. The cells were hand placed on the belt, although during Phase II (1994) the alignment system will be integrated with the ribbon handling system for automatically aligning and placing cells. Kester 2331 flux and thin (200  $\mu\text{m}$ ) Solec solar cells, 10.2 cm square, were used for soldering tests.

Soldering process parameters include the platen temperature for preheating cells and tabs, the voltage on the soldering lamps for heating the cells, the idle voltage on the soldering lamps, the heating time, and the cooling time. These parameters were adjusted until good solder joints were obtained. Soldered strings were produced by soldering cell front and back contacts simultaneously for the first time in November. The process parameters are listed in Table VI.

A number of cells soldered under the above listed conditions were subjected to pull tests to measure the force required to peel the ribbon from the cell. A Chatillon model DFG-10 digital force gauge was used to record the maximum force from each tab pulled. The results, provided in Table VII, show that good peel strengths have been achieved, averaging 690 g on the front contacts and 580 g on the back contacts. In many cases the solder joint was stronger than the silicon wafer, as the silicon broke and left the joint intact.

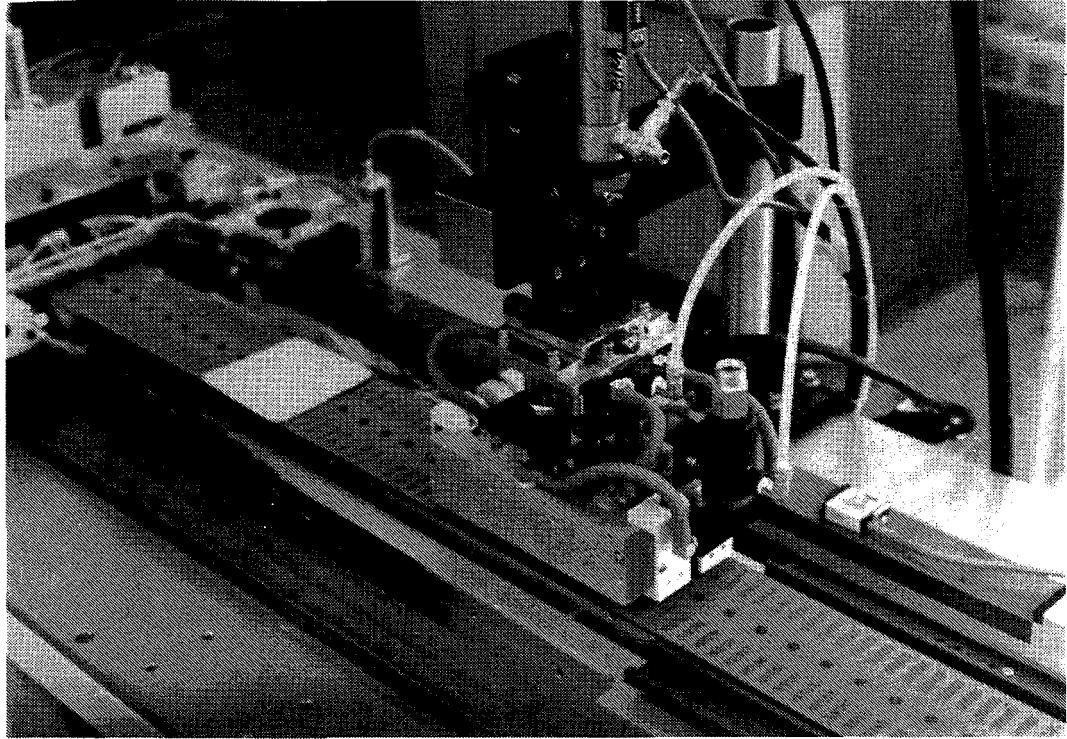


**Figure 22** *Photograph of solder head and actuator assemblies.*

**Table VI** *Initial process parameters for soldering cell strings.*

Parameter	Setting or Description
Platen temperature	85°C
Lamp voltage, heating	170 VAC
Lamp voltage, idle	35 VAC
Heating time	1.0s
Cooling time	1.5s
Cell type	Solec, 10.2 cm square, 200 $\mu\text{m}$ Cz-Si thickness
Flux type	Kester 2331, diluted
Ribbon type	0.100" x 0.003" Cu with Sn <sub>60</sub> Pb <sub>40</sub> coating

Platen heater tests showed that the maximum platen temperature obtainable with the two 1 kW heaters is approximately 85°C, due to the cooling effect of the vacuum blower. Since it is undesirable to operate at the upper temperature limit which the heaters can produce, higher power (2 kW) heaters were ordered and installed. These heaters also allow the investigation of soldering processes at higher platen temperatures, since higher cell preheat temperatures could potentially reduce the thermal shock on the cells during soldering.

**Table VII** *Solder joint pull test results. Pull angle = 45°.*

Test No.	Pull Force (kg)	
	Front Contact	Back Contact
1	0.50*	0.64*
2	0.76	0.64*
3	0.48	0.52*
4	1.09*	0.32*
5	0.61	0.68*
6	0.68	0.69*
Average	0.69	0.58
Std. Dev.	0.22	0.14

*\*Cell broke with solder joint intact during pull test.*

The higher power heaters allowed platen temperatures up to 145°C to be obtained. Tests with thin (~200 μm) Solec cells at this platen temperature resulted in incomplete solder joints on the cells' front contacts (under the cells, since they are face down), as if the joints were insufficiently heated. Increasing the solder lamp power made matters worse, resulting in overheated (highly oxidized) cell back solder joints, while the front contact joints were still incomplete. Careful observations during soldering showed that the belt was being curled by thermal expansion as it was heated by the platen, such that the belt surface became wavy and could not be held flat against the platen by vacuum, even with a cell in place on the belt. Thus cells were only in partial contact with the belt and with the tabs under the cells. The cell backs were still being radiantly heated by the solder lamp, but the cell could not transfer heat adequately to the front tabs except in the few places where the cell was in direct contact with the tabs. To solve the problem, the platen temperature was reduced to 80°C, at which point the vacuum can easily hold the belt flat against the platen. Tests done at this temperature produced good solder joints on both front and back contacts.

Another strategy was evaluated for reducing thermal stress on thin cells during soldering: the lamp heating time was increased to allow the use of a gentler, lower power heating cycle. The heating time was increased from 1.0s to 2.0s and the lamp heating voltage was reduced from 170V in 10V increments until, at 120V, there was insufficient heating to produce reliable solder joints. To provide a safety margin, the lamp voltage was set at 135V, or 5V above the lowest value at which good soldering occurred. The new set of parameters, listed in Table VIII, was used to fabricate four strings of nine cells each that were delivered to NREL in December. Note that the total heating-cooling cycle, at 3.0s, is well under the 4.0 s/cell goal for process throughput. A full second is still available for actuating the solder head and indexing the conveyor belt.

**Table VIII** *Parameters for soldering cell strings at lower lamp power.*

Parameter	Setting or Description
Platen temperature	80°C
Lamp voltage, heating	135 VAC
Lamp voltage, idle	25 VAC
Heating time	2.0s
Cooling time	1.0s
Cell type	Solec, 10.2 cm square, 200 μm Cz-Si thickness
Flux type	Kester 2331, diluted
Ribbon type	0.100" x 0.003" Cu with Sn <sub>60</sub> Pb <sub>40</sub> coating

During the soldering experiments, the automated ribbon handling system was operated for extended periods under string assembly conditions for the first time. Several adjustments and improvements were made to the system. The tab length and placement position were corrected through software adjustments. The indexing constant (also in software) for the conveyor belt stepper motor was calibrated by measuring belt travel for a given number of motor steps. Tab spacing, solder head position, and belt tracking were corrected through mechanical adjustments.

Experience with the ribbon handling system also identified a number of minor problems which will be corrected early in 1994. These problems and the solutions being implemented are as follows:

- The cardboard disks used for the ribbon reels are generally not straight and can rub on the inside surfaces of the reel holders. When using the larger 38 cm diameter reels, this friction can cause the ribbon to slip in the drive rollers as the rollers attempt to pull ribbon from the reel. The holders will be machined to create clearance space for the reels.
- The accumulator proximity sensors at the bottom of the ribbon loop were found to be unreliable in sensing ribbon, occasionally causing ribbon to pile up in the accumulators. They will be replaced with optical sensors, which were tested in December and found to work well.
- The cushions on the ribbon cutter assembly have impact surface areas that are too large, resulting in significant noise and vibration during operation. Cushions with smaller surface areas were ordered and the assembly will be modified for mounting them. Cushions will also be added to the ribbon clamp and form assembly to reduce vibration.

- At the flux station, flux removed from the ribbons by the air dryers was accumulating on the base and leaking out at the seam between the base and the cover. Grooves will be machined into the base to drain the flux into the bath. The flux station's cover and first ribbon diverter will also be modified to simplify ribbon threading.

### 2.2.7 Task 7 - Cell String Handling Process Development

Cell string handling comprises two tasks: (1) handling cells and interconnect tabs as they are being assembled together to produce cell strings, and (2) transporting these strings to the I-V tester and to the array table for placement in module-size arrays. The development of processes for both of these tasks is described in this section.

The method for handling interconnect ribbons and cells as they are being assembled and soldered together is a critical part of the assembly process. Early in this program a conveyor belt system was conceived with a vacuum capability for securely holding fragile components and a heating capability for preheating cells prior to soldering. A sketch showing the important features of the conveyor assembly concept is provided in Figure 23.

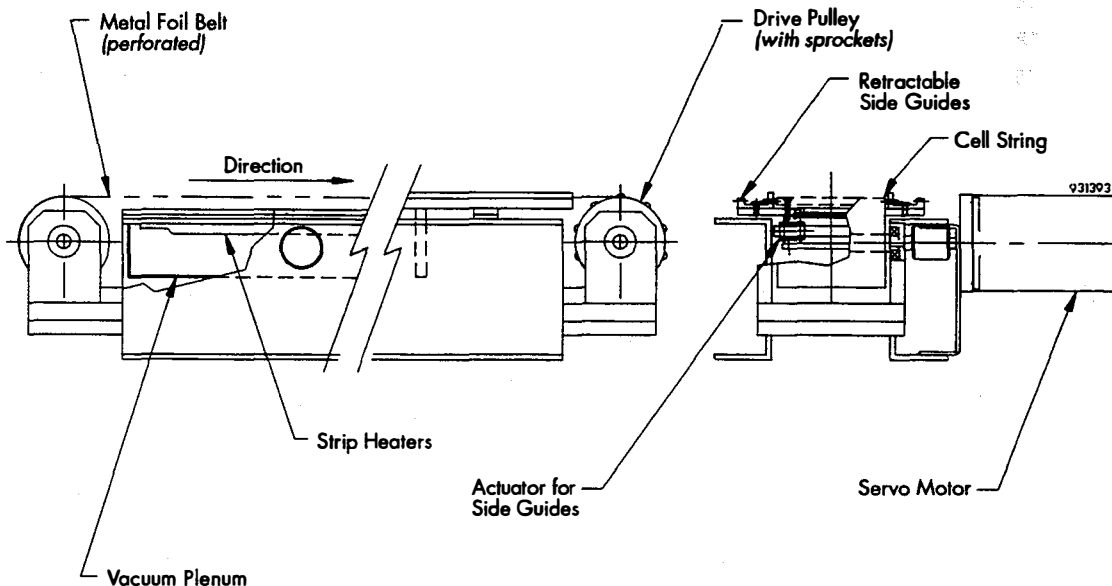


**Figure 23** *Cell string conveyor assembly.*

A heated vacuum platen was designed and fabricated to support the conveyor belt over its first 61 cm (24 inches). The platen is made of aluminum for low cost and high thermal conductance. Resistance strip heaters are mounted on the bottom surface of the platen, while a pattern of intersecting slots machined in the platen provides paths for air to flow from the conveyor belt perforations to a vacuum plenum below the platen. The plenum is a bent and welded sheet metal box which supports the platen. The plenum has a welded tube to allow connection to a source of high flow vacuum.

Initial testing was done in May on the vacuum platen subassembly. Two 500W resistance strip heaters were mounted to the bottom surface of the platen and the platen-heater assembly was mounted on the vacuum plenum. A thermocouple was installed in the platen and attached, along with the heaters, to a temperature controller. Initial testing showed that the heater power was inadequate, since the platen temperature was limited to approximately 80°C with moderate air flow through the vacuum holes. As a result, two 1000 W strip heaters were obtained. Tests with these heaters and with 2 kW heaters are described in Section 2.2.6.

Once the cells are soldered to the interconnecting tabs, the conveyor belt carries them out of the heated and vacuum-ported zone defined by the platen. Since the belt is quite long (~3 m total) to allow the assembly of 2m long strings, retractable side guides were designed to keep the cells in a straight line. The guides are retracted away from the cells when the belt indexes to prevent contact with the cell edges. When the belt stops, the guides move slowly towards the cells to a preset limit, then quickly retract before the next belt motion.

Before a commitment was made to invest in the tooling and expense of a full length belt and pulleys, a 91 cm (3 ft) long prototype belt section was fabricated to test the effectiveness of the vacuum hole pattern in holding cells and ribbons. This belt section was made of the same materials and has the same vacuum hole and sprocket hole pattern required for the full length belt. A shop vacuum was attached to the plenum and tests were done with various ribbons and cells. The belt was found to hold one or more cells very securely, either with or without ribbons. No motion of the cells with respect to the belt was observed when the belt was moved rapidly over the platen surface. When only a pair of ribbons was placed on the belt, however, they were held weakly, indicating the need for a stronger source of vacuum. Thus a regenerative blower was obtained which generates lower pressures and higher flows than the shop vacuum.

Based on the positive results of the prototype belt test, a full length belt and pulleys were designed. The belt was ordered from a vendor who specializes in the fabrication of stainless steel belts. The belt is formed into a continuous loop by electron beam welding the steel, resulting in an extremely smooth seam. The belt was perforated with vacuum holes and with holes for mating with a sprocketed drive pulley. The sprockets ensure that the belt indexes with the accuracy needed to control cell spacing and tab placement. The belt was also coated with a Teflon<sup>®</sup> surface to reduce any tendency the flux might have to stick to the belt and for ease of cleaning.

Other details of the conveyor belt assembly were designed, fabricated, and assembled, including the pulley mounts and belt tracking mechanism, the retractable side guides, the side guide actuator mechanism, belt carrier plates, and conveyor structural elements. A stepper motor and controller for driving the belt was selected, ordered, and installed. The motor is coupled to the drive pulley with a flexible coupling and a 10:1 gear reducer to increase the belt indexing accuracy. The photograph in Figure 24 shows, from right to left, the stepper motor, gear reducer, motor mounting bracket, flexible coupling, pulley mount, and drive pulley. The conveyor belt, mounted on the pulley, has a central row of large holes that function both as vacuum holes for cells and sprocket holes for the spherical ball bearing sprocket teeth pressed into the drive pulley. Patterns of small vacuum holes on either side of the large central holes are used to hold the ribbons on the belt.

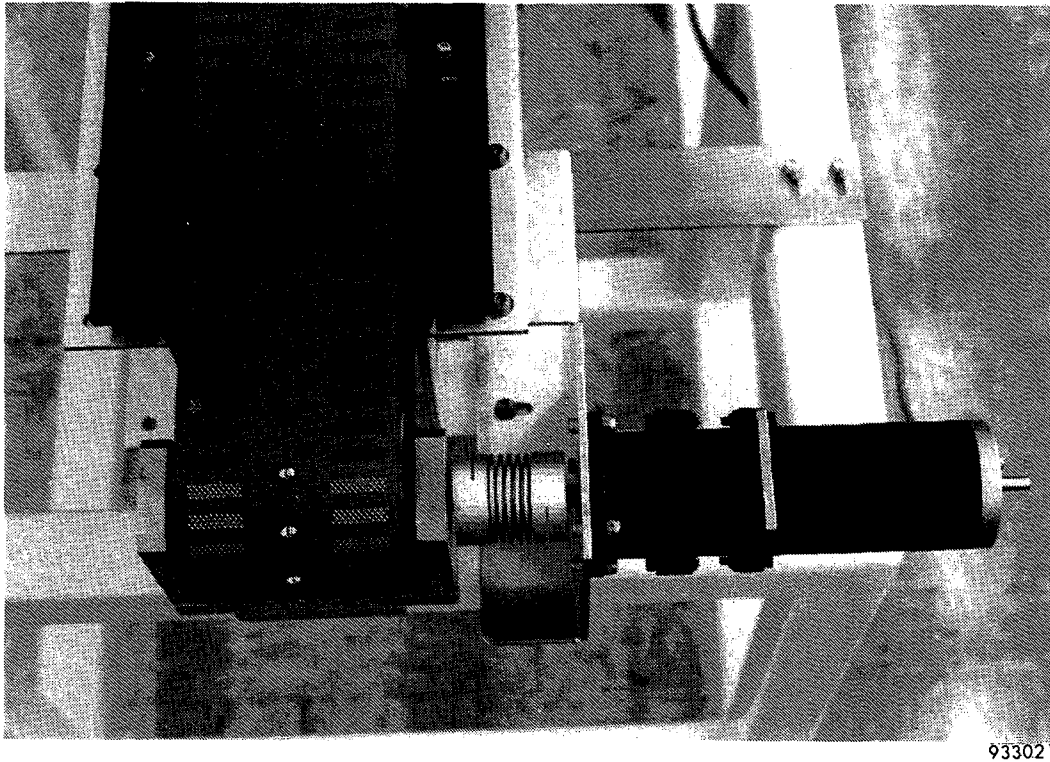


**Figure 24** *Drive pulley end of the vacuum conveyor belt.*

After the conveyor belt system was assembled, it was used along with the ribbon handling system for developing soldering processes, as described in Section 2.2.6, above. During this testing period it was noted that the vertical gap between the belt and the ribbon shuttle (which places the interconnect tabs on the belt) was larger than necessary. The height of the conveyor belt was raised to reduce the gap by 2.5 cm, thereby improving the accuracy and repeatability of tab placement.

When a cell string is completed, it is picked up from the conveyor belt by a string transfer mechanism. The mechanism consists of a linear array of vacuum pick-ups suspended from a four-axis manipulator, as shown in the drawing in Figure 25. After picking up the cell string, the mechanism carries it to the in-line I-V tester for an electrical performance test, and then places the string either on the array table, if the string passes the test, or on the reject table. The lay-out drawing of the complete system (Figure 3) shows a plan view of the cell string conveyor, the string transfer mechanism, the string I-V tester, the string array table, and the reject string table. The system is designed with the capacity to assemble groups of cell strings up to 2.0m long by 1.4m wide on the string array table.

The string transfer mechanism design was completed and components were purchased, fabricated, and assembled. A large structural frame was designed for supporting the string transfer mechanism and a number of other assemblies, including the drive end of the string conveyor, the in-line string I-V tester, the array table, and the reject table. The frame, the array table, and the reject table were fabricated and are shown in the photograph in Figure 26. Work on the I-V tester is continuing, with completion scheduled for 1994 (see Section 2.2.8).

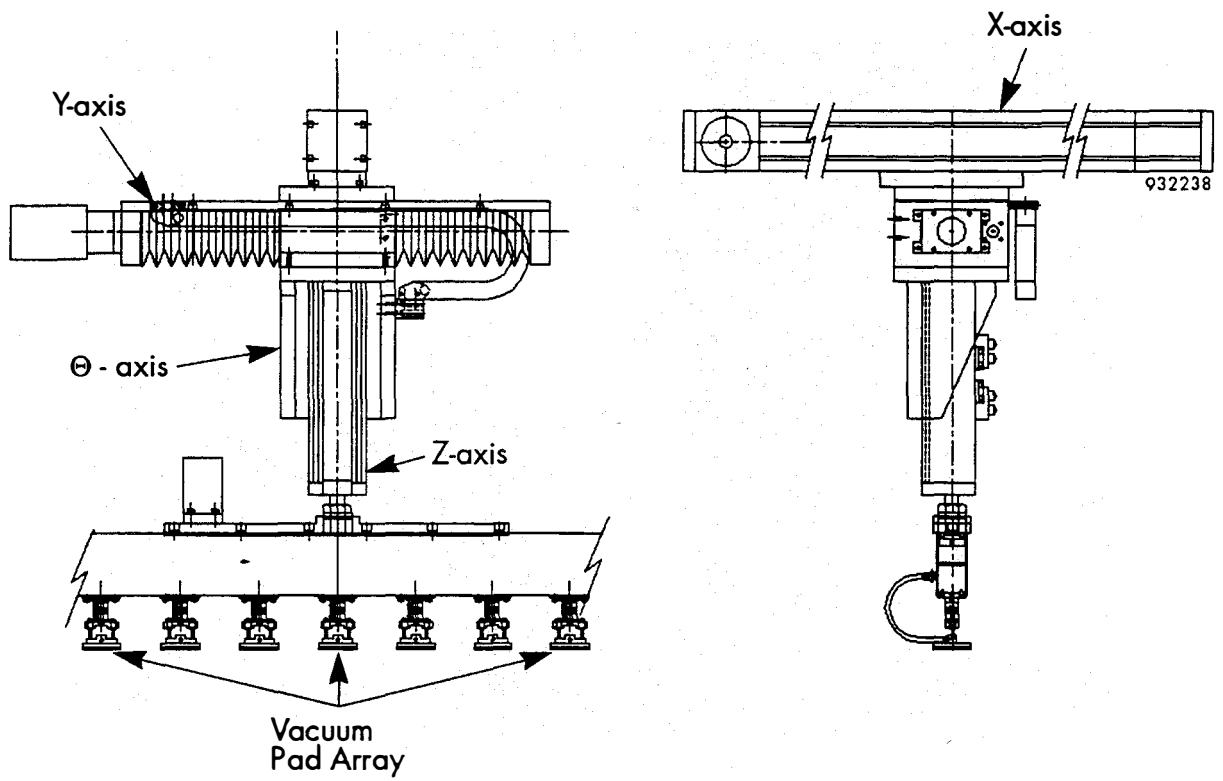


**Figure 25** *Cell string transfer assembly.*

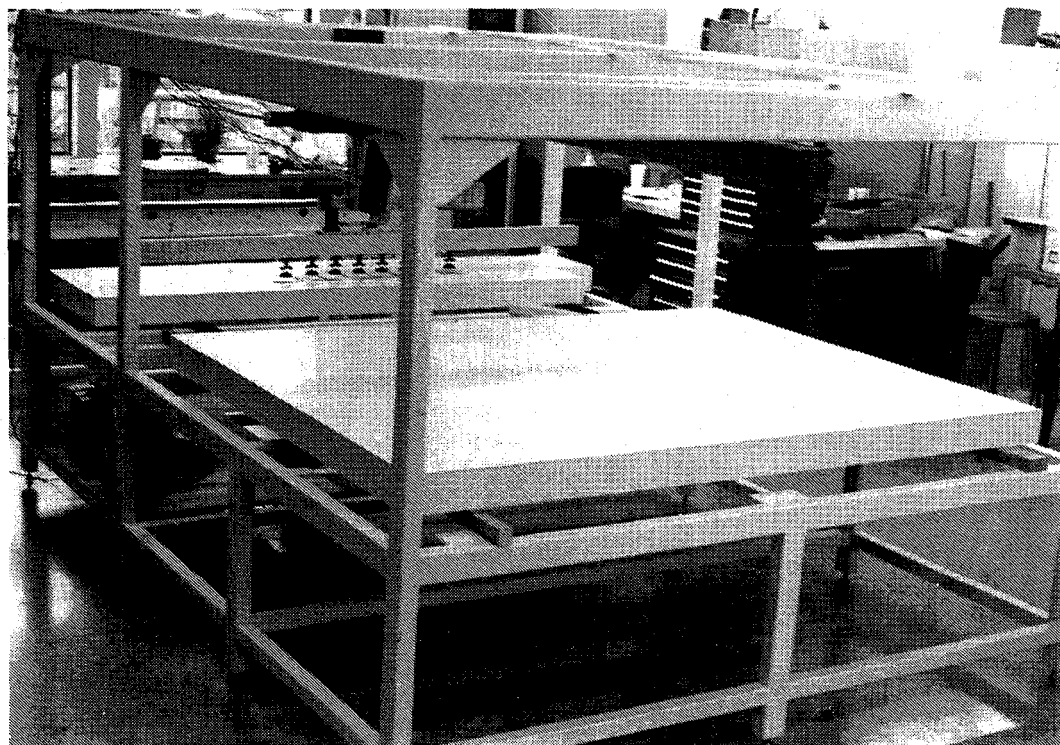


**Figure 26** *Frame for string transfer mechanism, conveyor, I-V tester, and tables for cell string arrays (foreground) and reject strings (background).*

The cell string manipulator provides string motion in four axes (x, y, z, and  $\theta$ ). Pneumatic z and  $\theta$  actuators provide 2.5 cm of z motion and 180° of  $\theta$  motion. The z motion is used to pick up and place the cell string, while the  $\theta$  motion allows strings to be placed in alternating plus and minus orientations, a standard technique used for arranging strings in series. Adjustable position stops are provided for both ends of the  $\theta$  travel. Both  $\theta$  and z axes are equipped with position sensors.

The y axis has fairly short travel (20 cm) driven by a ball screw type of positioner and a stepper motor, similar to those used on the cell aligner. Y motion is used if an offset in the string length direction is desired, as is normally the case for round cells.

A belt driven linear positioner is used for the long x motion (2.44m). The x motion is used to transport a string from the conveyor to the I-V tester and then to either the string array table (good string) or the reject table (reject string). A stepper motor drives a toothed belt that moves a stage along ball bearing ways. The load carried by the x axis stage is sufficiently massive that a 6:1 gear reducer is used to lower the torque requirements for the stepper motor.

An array of vacuum pick-ups is suspended from the 4-axis manipulator. The pick-ups are supported by a two meter long channel designed to allow placement of the pick-ups anywhere along the length of the channel. One pick-up is used for each cell in a string. The pick-ups are of the same floating design used by the cell loader and the cell aligner.

The x, y, z, and  $\theta$  actuators for the cell string transfer mechanism were assembled together in November and mounted on the frame. Stepper motors were mounted on the x and y axes and connected to motor controllers. The x and y controllers and actuators were tested by downloading commands from a personal computer to the stepper motors via the motor controllers. Both axes are functioning properly.

The vacuum pick-up array, vacuum manifold, vacuum pump, and rotation stops were mounted to the manipulator. Temporary air line connections were made to test the  $\theta$  and z actuators, which are functioning properly. A photograph of the string transfer mechanism is shown in Figure 27. Various components were ordered to complete the pneumatic system, including solenoid valves, filters, regulators, lubricators, and gauges.

#### 2.2.8 Task 8 - In-Line I-V String Testing Development

The need for an illuminated cell string performance test for in-line quality control after string soldering was recommended to Spire by module manufacturers during the Task 1 design definition efforts. As a result, Task 8 was added to Phase I of the program, starting in July, 1993. This work continues in Phase II as Task 13.

The in-line string I-V tester measures string electrical performance under simulated sunlight and compares the measured data with one or more acceptance criteria to determine if the string should be used in a module. For example, measured values for string open circuit voltage, short circuit current, and maximum power can be compared to minimum acceptance values preselected by the operator; if any one of the three measured values does not meet or exceed the acceptance value, the string will be placed on the reject table.

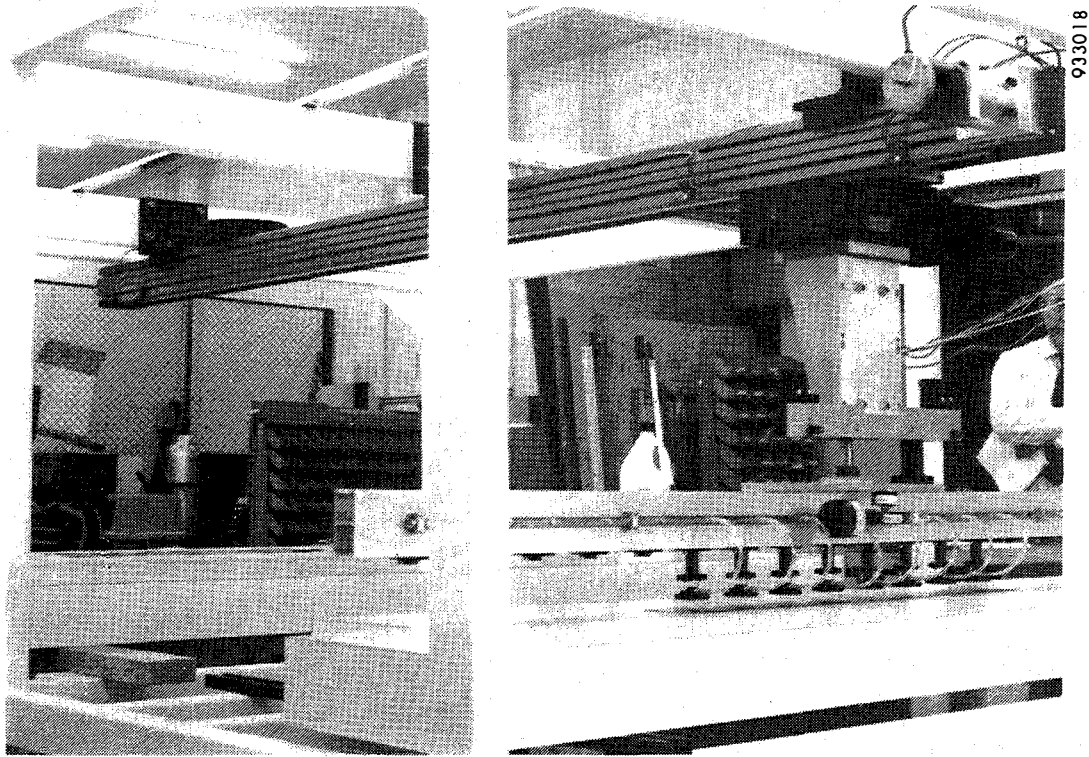


**Figure 27** *String transfer assembly, including the 4-axis manipulator and the cell string vacuum pick-up array.*

The in-line string I-V tester comprises a xenon light source, optics, power supply, and pulse forming network for producing a uniform one-sun illumination on the cell string; a calibrated reference cell for monitoring the lamp intensity and triggering the measurement; test probes for making contact to the string; an electronic load for sweeping the I-V curve; and a personal computer for controlling the light source, acquiring, analyzing, displaying, and storing data, and comparing string performance with stored pass/fail criteria.

The design of the lamp assembly and the simulator enclosure was completed in November. A lay-out drawing is provided in Figure 28. The assembly has two 1 m long xenon arc lamps mounted end-to-end inside tubular glass spectral filters. Lamp mounts, filter mounts, electrical contacts, and cooling jets for the lamp seals were designed and ordered. The lamp mounts are designed to minimize the space between the lamps for illumination uniformity. The lamp assembly is mounted in a sheet metal pan that attaches to the bottom of the main simulator enclosure. The enclosure has access panels for servicing the lamps, while the pan and lamp assembly can be removed as a unit if necessary.

A detailed design was completed for the probe assembly that will make electrical connections to the ends of a cell string. The design uses three spring-loaded contacts at each end of the cell string, two to collect current from the two interconnect tabs and one to sense voltage from one of the tabs, thus providing a four-point (+V, -V, +I, -I) probe arrangement for maximum measurement accuracy.

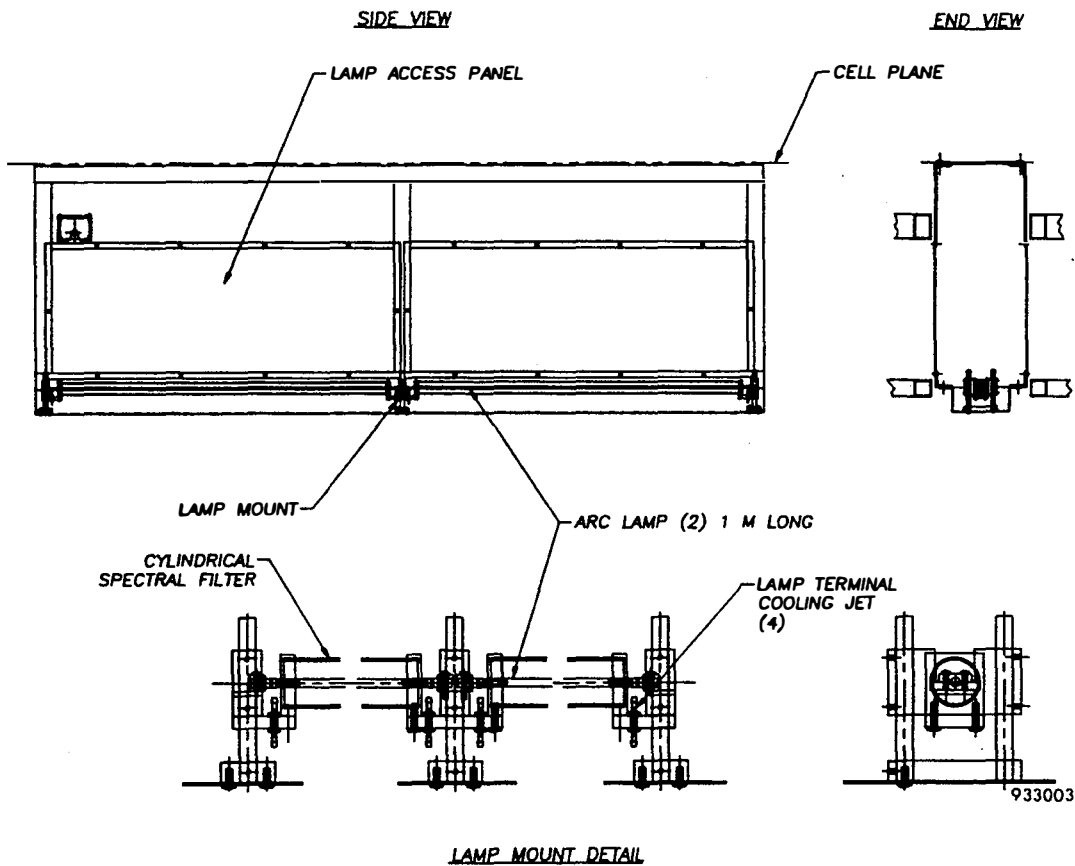


**Figure 28** *I-V tester sun simulator enclosure and lamp assembly.*

The I-V testing process involves placing a cell string on the glass test stage (above the sun simulator lamp) with the string transfer mechanism and then actuating two sets of contacts onto the tabs that extend from the ends of the string. The initial concept for contacting the tabs had a mechanism at each end of the cell string to move the probes onto the tabs. Problems were encountered in the design of the contact mechanism, however, due to the limited clearance for actuating the contacts under the string transfer mechanism and the potential for interference with vacuum pick-up pads suspended from the transfer mechanism.

An alternate method was then devised in which the probes are attached to the beam on the string transfer mechanism. This design solves the interference problems and eliminates the two actuators (one at each end of the cell string) for the contact assemblies, since the z-motion of the beam is used to press the contacts onto the tabs. A lay-out drawing of this probe assembly is provided in Figure 29. Note that two additional spring contacts have been added at each end of the string to carry the current and voltage signals to the electronic load. This greatly shortens the four measurement wires that would otherwise have to be routed through the cable ways used by the transfer mechanism.

The two contact assemblies can be mounted anywhere along the beam. Brackets with slots have been designed for adjusting the contact spacing and the contact height. The two contact block assemblies are mounted on a track that extends along the full length of the glass stage to allow alignment to the contact assemblies.

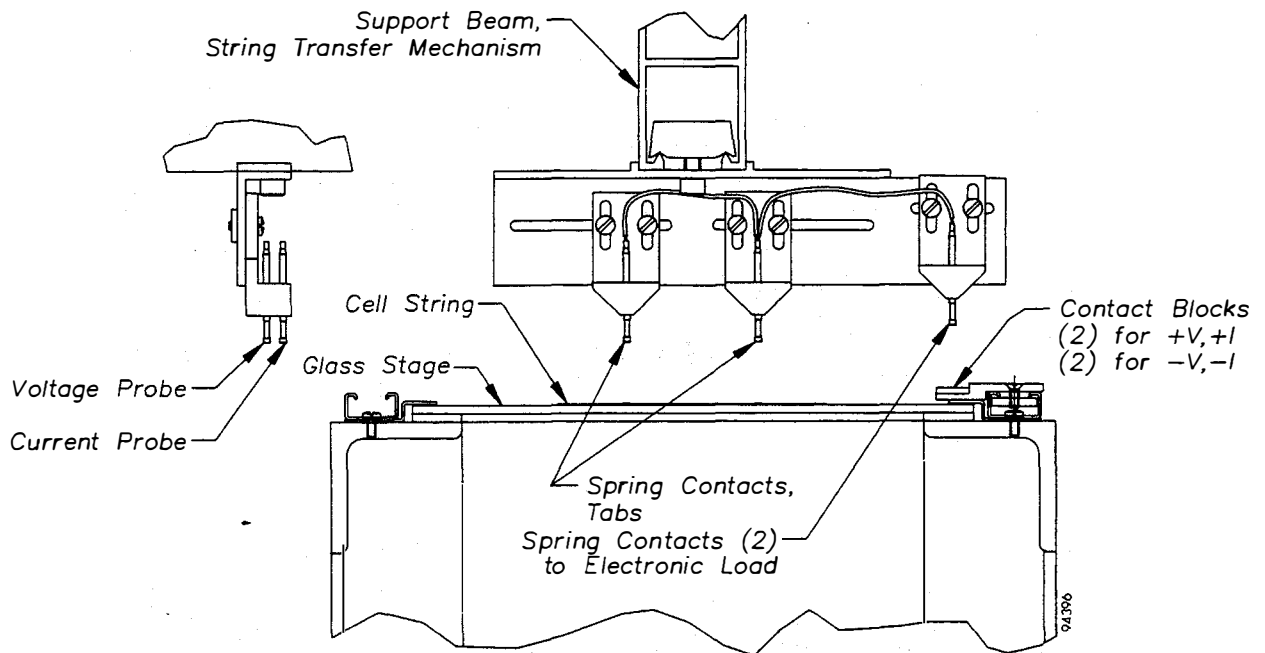


**Figure 29** *Contact probe assembly, in-line I-V tester. Identical contact assemblies and contact block assemblies are mounted at each end of the cell string.*

Components for the lamp assembly, the lamp enclosure, and the probe assembly were ordered or released for fabrication. The xenon lamps, a high voltage power supply for the lamps, and a power supply for the electronic load were ordered and received. The lamps are the same type used in Spire's SPI-SUN SIMULATOR™ 660 module tester, which has uniform irradiance over a 2m by 2m test plane.

A new lamp pulse forming network will be designed to increase string testing throughput. In Spire's present sun simulators, used for module testing, the lamps flash repetitively at 15 Hz, and one datum point on the I-V curve is measured during each flash. Thus it takes approximately 17s to complete an I-V curve consisting of 256 data points. Throughput can be increased without a significant loss in accuracy by reducing the number of data points to 100, which requires a measurement time of 6.7s. However, a different approach will be taken to maximize throughput: a long flat light pulse will be generated and the complete I-V curve will be measured in a single pulse. The pulse length will be approximately 5 to 10 milliseconds long.

### 2.2.9 Tasks 9 and 10 - Process Subassembly Design and Test

The design and test of process subassemblies is described in detail in the above process development sections (Sections 2.2.1 through 2.2.8). Design work that was completed at the end of December includes the mechanical design of subassemblies for cell loading, cell aligning, interconnect ribbon handling, ribbon fluxing; ribbon to cell soldering, cell string handling, and in-line I-V string testing. Each subassembly comprises a number of lower-level subassemblies which are listed in Table IX.

**Table IX** *Subassemblies, automated solar cell assembler.*

Process subassembly	Lower-level subassemblies
Cell loading	Cell stack carriers Carrier shuttle Load and reject stack elevators Two axis pick-and-place manipulator Vacuum end-effector
Cell aligning	Four axis robotic manipulator Vacuum end-effector Video imaging and processing system
Interconnect ribbon handling	Ribbon reels Ribbon accumulators Ribbon clamp and form assembly Ribbon cutting assembly Ribbon shuttle
Ribbon flux application	Flux station Ribbon drive rollers Automatic flux filling system
Ribbon to cell soldering	Two lamp solder head Actuator assembly
Cell string handling	String conveyor Heated vacuum plenum Four axis manipulator Vacuum end-effectors assembly String array table and reject string table
In-line I-V string testing	Sun simulator Test probes assembly Electronic load and measurements

Electrical and pneumatic controls have been designed for each of these subassemblies with the exception of the in-line string I-V tester. The electrical design for the I-V tester will be completed in the first quarter of 1994. A personal computer with an Intel 486-DX microprocessor was procured for software development tasks. The computer will also provide overall system control and operator interface functions for the integrated system. An Allen Bradley programmable logic controller (PLC) was also ordered and installed for system control purposes.

#### 2.2.10 Task 11 - Integrated System Design

Under this task an integrated system is being designed in which the individual process subassemblies will be combined to form a single automated system. Integration is required for the mechanical subassemblies and for the pneumatic, electrical, and software systems used for powering and controlling the subassemblies.

Mechanically, all of the process subassemblies listed in Table IX, above, are designed to mount together on three structural frames which join together to form a single system. One frame supports the loader and aligner subassemblies; the second frame supports the ribbon handling subassemblies, the flux application subassembly, the cell soldering subassembly, and one end of the string conveyor subassembly; the third frame supports the string handling subassemblies, including the other end of the string conveyor, and the I-V tester subassembly.

Three pneumatic distribution manifolds have been designed, one for each of the three structural frames. These manifolds will supply the subassemblies with filtered compressed air at the proper pressures and flows. Lubricators will be installed on the lines that supply air to actuators for which lubrication is recommended. Pressure switches will be installed on critical regulators to signal the control system when the air pressure drops below the level needed for proper operation.

Electrical systems have been designed, including the AC power system and wiring for communications between subassemblies. Both the main power distribution box and the PLC, which controls much of the system operation, are mounted in the centrally-located frame that supports the ribbon handling subassemblies. AC outlet boxes and connectors for signal lines will be provided in two locations on the ribbon handling frame: where it joins to the loader/aligner frame and where it joins to the string handling/I-V tester frame.

A block diagram of the control system is provided in Figure 30. A 486 PC will be used for overall system control and operator-machine interface functions, which include:

- user inputs, such as cell type, number of cells per string, number of strings per module, and I-V test acceptance criteria
- user commands for system control, such as run, pause, and reset
- machine outputs during operation, such as status messages (*e.g.*, cell carrier empty or string array completed) and error messages
- diagnostics when requested by the operator (string performance, cell yield, *etc.*).

Operator inputs and commands will be downloaded by the PC to the PLC, the cell aligner PC, and the I-V tester PC. The aligner PC will control the cell alignment subassemblies, the cell loader manipulator, and the loader vacuum end-effector. The I-V tester PC will control the I-V string tester subassemblies. The PLC will control the operations of the remaining subassemblies.

#### 2.2.11 Task 12 - Information Dissemination

A news release was prepared by Spire and approved by NREL to announce the start of this program. Spire mailed the news release in March to 137 publications, including trade magazines, journals, and photovoltaic industry newsletters. The program was also mentioned in a May news release reporting on Spire's first quarter sales and earnings. As a result of these news releases, articles on this program appeared in several periodicals, including the March issue

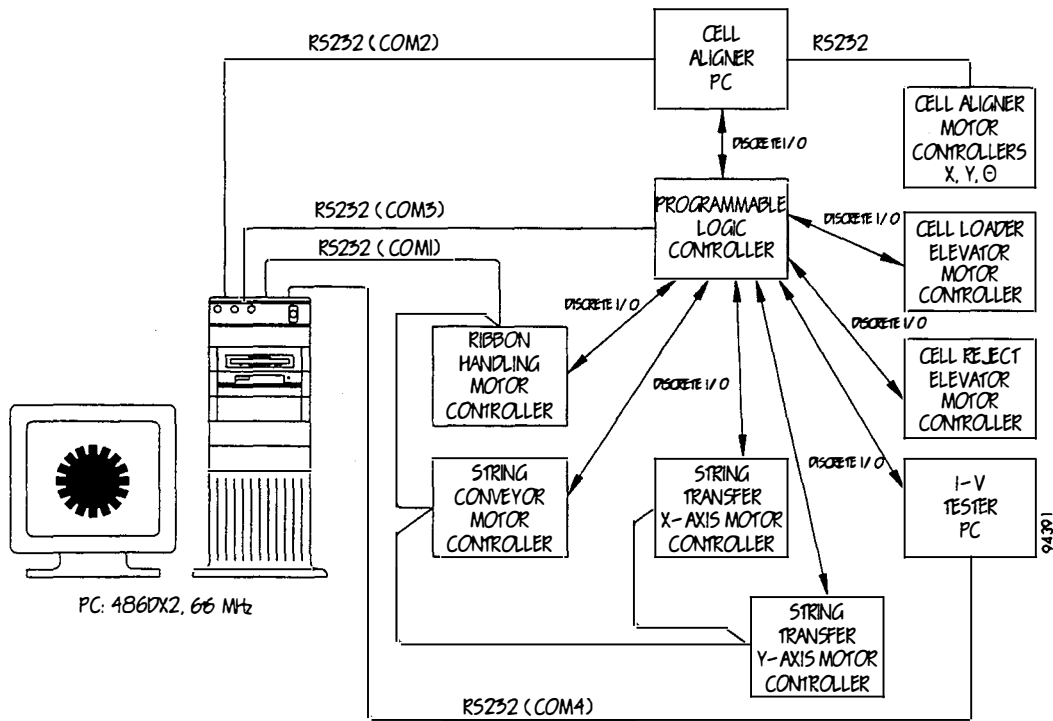


**Figure 30** Cell assembler control system block diagram.

of Independent Energy,<sup>4</sup> the April issue of Photovoltaic Insider's Report,<sup>5</sup> the May issue of PV News,<sup>6</sup> the May issue of Laser Focus World,<sup>7</sup> and second quarter 1993 issue of the Solar Industry Journal.<sup>8</sup>

Spire personnel (G. Darkazalli and R. Little) attended the Soltech 93 conference in Washington, D.C. On April 26, R. Little gave a five minute oral presentation on this program as part of the Industry Press Announcement session of the Solar Energy Forum.<sup>9</sup>

Spire engineers met with the engineers responsible for PV module manufacturing at Solec International, Siemens Solar Industries, Mobil Solar Energy Corporation, and Texas Instruments, as described in Section 2.2.1, above. In addition to the design definition activities carried out for Task 1, the discussions served to inform these manufacturers about Spire's ongoing activities and plans under this program.

A preliminary specification sheet was prepared to provide more detailed information to those manufacturers interested in automating their cell interconnecting processes. While the specifications are still preliminary, the general concepts and anticipated performance of the system are described. The system has been designated the SPI-ASSEMBLER™ 5000. The specification sheet has been distributed to a number of PV module manufacturers. A copy of the specification sheet, which was updated in November, is provided as Appendix A.

A plan view lay-out drawing of the complete system (provided in Figure 3, above) was created and updated several times as the subassembly designs have progressed. This drawing was provided to interested manufacturers as a supplement to the specification sheet. The drawing is annotated to label the major subassemblies.

Spire personnel (R. Little, G. Darkazalli, M. Nowlan, and S. Hogan) attended the IEEE Photovoltaic Specialists Conference in Louisville, KY, from May 10 to 14. A news release regarding the PVMaT-3A program was available at the Spire booth in the exhibits area. The program was discussed with personnel from several PV manufacturers, including Siemens Solar, Solarex, and Solec International.

A program review meeting was held for the PVMaT Technical Monitoring Team (TMT) at Spire on June 2. Attendees were the members of the TMT (D. Mooney and J. Burdick, NREL, and A. Maish, Sandia), Spire personnel involved in the program (G. Darkazalli, M. Nowlan, S. Hogan, S. Sutherland, J. Murach, W. Breen, S. Rehtoris, and D. VanAmburg), and U. Mass. Lowell personnel involved in the program (P. Krolak, J. Milstein, and C. Kosta). Program progress and system design concepts were reviewed in detail. A tour of Spire's facilities was conducted, and subassembly components were examined.

A paper describing the processes being developed in this program was written and presented by M. Nowlan of Spire at the 12th NREL PV Program Review Meeting in Denver, CO, on October 14.<sup>10</sup> The paper will be published in the American Institute of Physics' conference proceedings series.

In November, a VHS videotape showing the operation of the process subassemblies being developed under this program was filmed and edited. Videotape of the loader and aligner assemblies was recorded at UML, while the ribbon and string handling assemblies were recorded at Spire. Recording and editing of the final tape was done by E. Babcock of the audio-visual lab at the College of Engineering at UML. Two copies were sent to NREL and other copies were retained by Spire for showing to PV manufacturers.

S. Hogan of Spire attended the 7th International Photovoltaic Science and Engineering Conference held in Nagoya, Japan, November 22 to 26. The videotape was shown and copies of the preliminary specification sheet were provided to a number of manufacturers from the U.S. (including Solarex and Texas Instruments) and other countries.

On December 2, the First Annual Program Review Meeting was held for this program at NREL in Golden, CO. In attendance were the TMT members (as above but with H. Thomas replacing D. Mooney), E. Witt, R. Mitchell, and others from NREL, and M. Nowlan from Spire. Videotapes were shown to illustrate the differences between Spire's previous cell tabbing and connecting processes and the new processes being developed in this program. A viewgraph presentation was given by M. Nowlan to describe the progress made from January through the end of November, 1993.

### 2.3 Thin Solar Cells

A supply of solar cells was obtained to evaluate the ability of the subassemblies to process thin cells without significant cell breakage or other damage. As part of Solec's lower-tier subcontract, they fabricated and delivered 1000 thin solar cells (200  $\mu\text{m}$  silicon thickness) for this purpose during Phase I. These cells were used to evaluate the cell loading process, the cell alignment process, the solder flux application process, the ribbon to cell solder process, and the cell string handling process.

## SECTION 3 CONCLUSIONS

As part of the PVMaT Phase 3A project, Spire and its team members are working on a program titled "Automated Solar Cell Assembly Teamed Process Research." The team members include lower-tier subcontractors Solec International, a PV module manufacturer, and the University of Massachusetts Lowell's Center for Productivity Enhancement, automation experts.

The program objective is to develop high yield, high throughput, fully automated processes for tabbing and interconnecting thin silicon solar cells. More specifically, our goals are to process cells at a rate (4.0 s/cell) that is twice as fast as current systems, to significantly reduce the labor required by combining tabbing and interconnecting into a single automated process, and to handle cells fabricated from much thinner silicon wafers (200  $\mu\text{m}$ ) than current systems can handle with high yield.

Highlights of the first year of the program are as follows:

**Task 1 - Design Definition** - Spire engineers met with Solec to determine their specific needs for cell interconnection, and with other PV module manufacturers (Siemens Solar, Mobil Solar, and Texas Instruments) to determine the generic needs of the PV industry. Data were collected on the manufacturers' cell characteristics, interconnect ribbon characteristics, solder flux or paste requirements, and other factors (Table II). These data were used to establish specifications for the process subassemblies, in terms of the sizes and types of materials to be processed. Another result of the discussions with PV manufacturers was the recommendation for an in-line string I-V test, which was subsequently added to the program as Tasks 8 and 13. This quality control test will identify cell strings with poor performance prior to module assembly, thus reducing rejects and improving module quality.

**Task 2 - Cell Loading Process Development** - An extensive survey of commercial wafer handling equipment was conducted. R- $\theta$ -z wafer robots, common in the semiconductor industry, were found to be too slow to meet our 4 s/cell requirement. Carriers for cell stacks have been selected over slotted cassettes because of the greatly reduced volume and frequency of carrier loading. A two stack system has been selected to allow continuous cell feeding (no interruptions for the operator to load a stack) for higher throughput. Commercial stack unloaders could not satisfy all of the requirements for speed, cell size capacity, and dual stack capability, so a custom system was designed and built. A special vacuum pick-up end effector with a floating mount was also designed and fabricated for handling thin cells.

**Task 3 - Cell Alignment Process Development** - An alignment process algorithm has been formulated (Table IV). A four axis (x-y-z- $\theta$ ) motion system for aligning and transporting cells has been selected and installed. Stepper motors provide the required alignment accuracy in x, y, and  $\theta$ , while z is air actuated for reduced cost. A floating mount vacuum end effector, similar to the one designed for cell loading, is installed on the motion system. A video camera, lighting, and alignment software are being tested. Images of cell contact patterns have been obtained, but problems in reliably detecting cell edges have been encountered, due to the optically noisy ambient background above the cell. Experiments with lighting and white backgrounds will be done in early 1994.

**Task 4 - Interconnect Ribbon Handling Process Development** - The mechanical design and fabrication of processing subassemblies for ribbon handling, bending, and cutting have been completed. These subassemblies include the ribbon reels, the flux station (which includes the ribbon drive assemblies), the ribbon accumulators, the ribbon clamp and form assembly, the ribbon cutter, and the ribbon shuttle assembly. The subassemblies have been mounted on a common frame, connected to a programmable logic controller, and operated together as a fully integrated and automated ribbon handling system.

**Task 5 - Solder Flux Application Process Development** - A prototype interconnect ribbon fluxing subassembly was designed and fabricated. Preliminary trials done with a no-clean flux showed a tendency for the flux to stick the ribbon to the drive rollers. Squeegees were added and the roller material was changed without success. Air dryers were added which reduced the quantity of flux on the ribbon, and flux thinner was tried, but this type of flux still occasionally stuck to the rollers. Two other types of flux were tried; both fed without sticking, and one of these was successful in soldering to Solec cells (Table V). A revised flux station was designed and fabricated, with a vented cover for trapping and exhausting solvent fumes, and a float switch and peristaltic pump for automatically maintaining the proper flux level.

**Task 6 - Ribbon to Cell Solder Process Development** - Spire's light soldering process has been combined with conductive preheating to reduce thermal stress on the cells and increase throughput. Solder head and actuator assemblies were fabricated and installed over the heated vacuum conveyor. A process was developed which, for the first time, simultaneously solders interconnect tabs to cell front and back contacts. Pull tests show that good peel strengths have been achieved, averaging more than 500 g with a 45° pull angle (Table VII). Four strings of nine cells each were soldered and delivered to NREL in December. The ribbon handling, ribbon fluxing, belt indexing, and soldering processes were all done automatically. The soldering cycle used for these strings was 3.0 s/cell (Table VIII).

**Task 7 - Cell String Handling Process Development** - A new concept for a heated vacuum conveyor belt was devised for holding and preheating cells and interconnect tabs as they are assembled and soldered together. A vacuum plenum, heated vacuum platen, and a prototype perforated conveyor belt were designed, fabricated, and used for testing the feasibility of the concept. The positive results of this testing resulted in the design and fabrication of a full length (3.05 m) conveyor belt assembly. Testing also indicated the need for higher power platen heaters and a high flow vacuum blower, which were obtained and installed in the full scale system. The system was successfully used to produce the cell strings delivered to NREL in December. A string transfer mechanism, comprising a linear array of vacuum pick-ups suspended from a four axis manipulator, was designed for picking up strings from the conveyor belt and transporting it to the in-line I-V tester and the string array table or the string reject table. The mechanism's components have been fabricated, installed, and tested for proper operation. Software for automatic operation will be developed in 1994.

**Task 8 - In-Line I-V String Testing Development** - An in-line I-V string tester is being designed and fabricated for measuring the performance of soldered cell strings under simulated sunlight. Strings up to 15 cm wide by 200 cm long will be tested. The tester comprises a filtered pulsed xenon light source, lamp power supply, reference cell, test probes, electronic load, and computer for control and data acquisition. Components for the lamp assembly, lamp

enclosure, and probe assembly were designed and ordered. The xenon lamps, power supplies for the lamps and the electronic load, and components for the reference cell assembly were ordered and received. A new lamp pulse forming network will be designed for maximum testing throughput; the entire I-V curve will be measured in a single 5 to 10 millisecond light pulse. Electrical and software development will continue in 1994 under task 13.

**Task 9 and 10 - Process Subassembly Design and Test** - The mechanical design for the individual process subassemblies is completed for all cell assembler functions: cell loading, cell aligning, interconnect ribbon handling, ribbon flux application, ribbon to cell soldering, cell string handling, and in-line I-V string testing. The major and lower-level subassemblies are listed in Table IX. Remaining work includes software for automatic control of the cell loader; testing of the cell loader's air knives; testing of the video camera and lighting system for detecting cell edges; software development for aligning and inspecting cells; electrical and software design and testing for the I-V string tester; and software for automatic control of the string manipulator.

**Task 11 - Integrated System Design** - Mechanical, electrical, and pneumatic systems were designed to mount on three structural frames for integrating the individual process subassemblies. These frames in turn join together to form a single fully automated system. A personal computer will provide overall system control and operator-machine interface functions.

**Task 12 - Information Dissemination** - Spire mailed a news release to 137 publications to announce the start of this program to the PV industry. As a result, articles have appeared in at least five industry news letters and magazines. A preliminary specification sheet (Appendix A) and an annotated lay-out drawing (Figure 3) were prepared which describe the complete system, which has been named the SPI-ASSEMBLER™ 5000. Copies of the specification sheet and drawing are being distributed to interested manufacturers. In April, Spire gave an oral presentation describing this program at Soltech 93 in Washington, DC. In May, Spire personnel met with a large number of PV manufacturers attending the IEEE Photovoltaic Specialists Conference in Louisville, KY. Spire engineers have visited Solec and Siemens Solar, and engineers from Mobil Solar and Texas Instruments have visited Spire to discuss the processes and systems being developed in this program. A design review was held for the PVMaT Technical Monitoring Team at Spire in June. A paper describing the processes being developed in this program was presented by Spire at the 12th NREL PV Program Review Meeting in Denver, CO, in October. In November, a videotape was filmed of the process subassemblies in operation. Copies were sent to NREL and retained by Spire to show to PV manufacturers. Spire attended the 7th International Photovoltaic Science and Engineering Conference held in Nagoya, Japan, in November, where the cell assembly system was discussed with a number of manufacturers from the U.S. and other countries. In December, the First Annual Program Review Meeting was held at NREL in Golden, CO, at which Spire presented a review of the progress made from January through the end of November, 1993.

#### SECTION 4 REFERENCES

1. P.D. Maycock, "World Module Shipments by Cell Technology," *PV News* **13** No. 2 (1994).
2. Spire Corporation, "Photovoltaic Manufacturing Technology Program," Phase I Final Report, SERI Contract XC-1-10057-1 (1991).
3. Fluoroware Wafer Carrier No. PA92-39M-0603 for 100 mm square solar cells.
4. K. Sheinkopf, "Advancing Photovoltaics," *Independent Energy*, March, 1993, 62.
5. R. Curry, "Spire Gets Contract to Develop High Throughput Processes Using Thin Solar Cells," *Photovoltaic Insider's Report XII* No. 4 (1993).
6. P. Maycock, "Spire Corporation Developing a 5 MW per Year Cell Interconnection Machine," *PV News* **12** No. 5 (1993) 6.
7. Y.A. Carts, "Spire Awarded \$1.2 Million Contract for Photovoltaic Manufacturing," *Laser Focus World*, May, 1993, 57.
8. "Industry News," *Solar Industry Journal*, Second Quarter, 1993, 12.
9. R. Little, "Automated Solar Cell Assembly Teamed Process Research," presented at Soltech 93, Solar Energy Forum, Washington DC, April 1993.
10. M.J. Nowlan, S.J. Hogan, S.F. Sutherland, W.F. Breen, J.M. Murach, and G. Darkazalli, "Development of Advanced Automation Processes for Photovoltaic Module Manufacturing," proc. 12th NREL PV Program Review Meeting, Denver, CO, October 13-15, 1993.

**APPENDIX A**  
**PRELIMINARY DATA SHEET**  
**SPI-ASSEMBLER™ 5000**

# SPI-ASSEMBLER™ 5000

## Automated Solar Cell Assembly

The Spire SPI-ASSEMBLER™ 5000 is an automated production machine which interconnects solar cells by soldering flat metal leads, or tabs, to cell contacts. The machine is designed to process standard or thin silicon cells with high throughput.

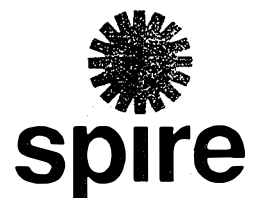
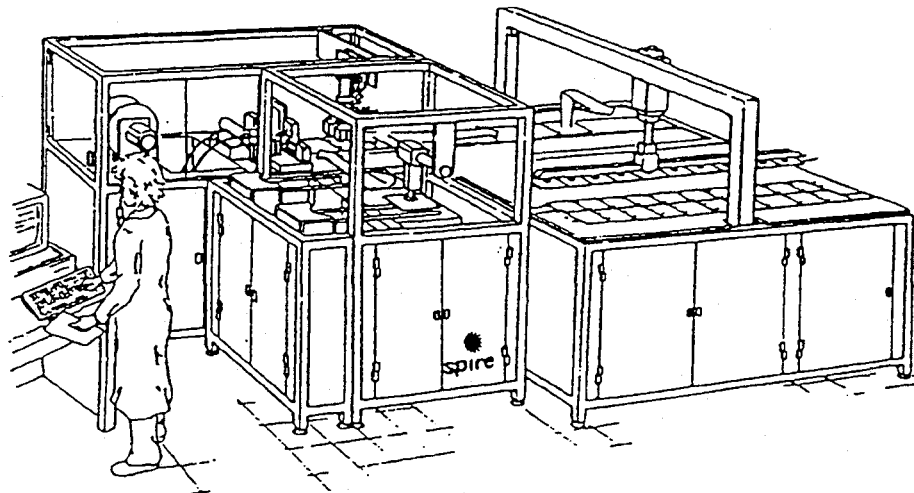
Solar cells are loaded and aligned with an optical pattern recognition system. Tab material is fed from reels, cut to length, and provided with a stress-relief bend. Tabs and cells are aligned together for soldering.

High-intensity lamps in the solder head assembly provide radiant thermal energy to the cell and tabs. Both front and back cell contacts are soldered in a single heating step.

The number of cells per string, the number of strings per module, and the string orientation (for series or parallel connection) are software programmable. Each completed string is automatically placed in the proper position on a module registration board.

## Features and Benefits

- ▶ Automated and programmable cell string assembly results in reproducible, high quality soldered cell arrays
- ▶ Machine vision for cell inspection and alignment
- ▶ High-intensity light soldering for improved throughput and yield
  - Rapid soldering time
  - Minimum mechanical force on cell
  - Low thermal stress
  - Continuously soldered contacts
- ▶ Software selectable module design
  - Tab length and stress-relief bend location
  - Number of cells per string
  - Number of strings per module
  - Strings arranged in series or parallel configuration
- ▶ Adaptable to a wide range of cell and tab designs
- ▶ Controlled by a personal computer with a powerful graphics-based software package



---

## **Preliminary Specifications**

1. *Solar Cell Geometry* \_\_\_\_\_ square, rectangular, round, or round with flats
2. *Maximum Cell Dimensions* \_\_\_\_\_ 15 cm x 15 cm (6 in. x 6 in.)
3. *Minimum Cell Thickness* \_\_\_\_\_ 150  $\mu$ m (0.006 in.)
4. *Number of Interconnect Ribbons* \_\_\_\_\_ 2
5. *Maximum Number of Cells per String* \_\_\_\_\_ 20
6. *Maximum String Length* \_\_\_\_\_ 200 cm (78.7 in.)
7. *Nominal Throughput* \_\_\_\_\_ 15 cells/minute
8. *Equipment Dimensions (excluding computer system)*  
Width \_\_\_\_\_ 488 cm (192 in.)  
Depth \_\_\_\_\_ 315 cm (124 in.)  
Height \_\_\_\_\_ 180 cm (71 in.)
9. *Equipment Weight, Net* \_\_\_\_\_ to be determined
10. *Utilities Requirements*  
Electricity \_\_\_\_\_ to be determined  
Compressed Air  
Pressure \_\_\_\_\_ 500 - 700 kPa (80-100 psi)  
Flow \_\_\_\_\_ to be determined

---

## **Options**

► *String I-V Test*

- A pulsed xenon lamp illuminates the cell string (up to 15 cm x 200 cm), an I-V curve is measured, and the string is placed either in a reject bin or in the proper location for a module, based on user selected criteria.

---

*For additional information and application assistance, please call or fax the Photovoltaics Equipment Division.*

# REPORT DOCUMENTATION PAGE

*Form Approved*  
OMB NO. 0704-0188

Public reporting burden for this collection of information is estimated to average 1 hour per response, including the time for reviewing instructions, searching existing data sources, gathering and maintaining the data needed, and completing and reviewing the collection of information. Send comments regarding this burden estimate or any other aspect of this collection of information, including suggestions for reducing this burden, to Washington Headquarters Services, Directorate for Information Operations and Reports, 1215 Jefferson Davis Highway, Suite 1204, Arlington, VA 22202-4302, and to the Office of Management and Budget, Paperwork Reduction Project (0704-0188), Washington, DC 20503.

1. AGENCY USE ONLY (Leave blank)	2. REPORT DATE May 1994	3. REPORT TYPE AND DATES COVERED Annual Subcontract Report 1 January 1993 - 31 December 1993	
4. TITLE AND SUBTITLE  Automated Solar Cell Assembly Team Process Research		5. FUNDING NUMBERS  C: ZAG-3-11219-01  TA: PV450101	
6. AUTHOR(S)  M.J. Nowlan, S.J. Hogan, G. Darkazalli, W.F. Breen, J.M. Murach, S.F. Sutherland, J.S. Patterson		8. PERFORMING ORGANIZATION REPORT NUMBER	
7. PERFORMING ORGANIZATION NAME(S) AND ADDRESS(ES)  Spire Corporation One Patriots Park Bedford, MA 01730-2396		10. SPONSORING/MONITORING AGENCY REPORT NUMBER  TP-411-6769  DE94011819	
9. SPONSORING/MONITORING AGENCY NAME(S) AND ADDRESS(ES)  National Renewable Energy Laboratory 1617 Cole Blvd. Golden, CO 80401-3393		11. SUPPLEMENTARY NOTES  NREL Technical Monitor: H. Thomas	
12a. DISTRIBUTION/AVAILABILITY STATEMENT		12b. DISTRIBUTION CODE  UC-270	
13. ABSTRACT ( <i>Maximum 200 words</i> )  This report describes work done under the Photovoltaic Manufacturing Technology (PVMaT) project, Phase 3A, which addresses problems that are generic to the photovoltaic (PV) industry. Spire's objective during Phase 3A was to use its light soldering technology and experience to design and fabricate solar cell tabbing and interconnecting equipment to develop new, high-yield, high-throughput, fully automated processes for tabbing and interconnecting thin cells. Areas that were addressed include processing rates, process control, yield, throughput, material utilization efficiency, and increased use of automation. Spire teamed with Solec International, a PV module manufacturer, and the University of Massachusetts at Lowell's Center for Productivity Enhancement (CPE), automation specialists, who are lower-tier subcontractors. A number of other PV manufacturers, including Siemens Solar, Mobil Solar, Solar Web, and Texas Instruments, agreed to evaluate the processes developed under this program.			
14. SUBJECT TERMS  manufacturing ; automation ; process ; photovoltaics ; solar cells		15. NUMBER OF PAGES 56	
17. SECURITY CLASSIFICATION OF REPORT Unclassified		16. PRICE CODE A04	
18. SECURITY CLASSIFICATION OF THIS PAGE Unclassified	19. SECURITY CLASSIFICATION OF ABSTRACT Unclassified	20. LIMITATION OF ABSTRACT  UL	